Universiteit
Leiden
The Netherlands

Synthetic peptides as tools in chemical immunology

Doelman, W.

Citation
Doelman, W. (2023, February 9). *Synthetic peptides as tools in chemical immunology*. Retrieved from https://hdl.handle.net/1887/3563057

Version:	Publisher's Version
License:	Licence agreement concerning inclusion of doctoral thesis in the Institutional Repository of the University of Leiden
Downloaded from:	https://hdl.handle.net/1887/3563057

Note: To cite this publication please use the final published version (if applicable).

4

Synthesis of glycosylated and fluorescently labeled antigenic peptides for immune-receptor interaction studies

Part of this work was published as: Riera, R.; Hogervorst, T.P.; Doelman, W.; Ni, Y.; Pujals, S.; Bolli, E.; Codée, J.D.C.; van Kasteren, S.I.; Albertazzi, L. Single-Molecule Imaging of Glycan–Lectin Interactions on Cells with Glyco-PAINT. *Nat. Chem. Biol.* **2021**, *17* (12), 1281–1288

L. Verschoor and R.W.R van den Kieboom also contributed to the work presented in this chapter

Introduction

Glycans have a critical role in immune response modulation through their interaction with immune lectins.[1–3] Immune cells express a variety of such lectins – protein receptors for glycans – and use these to distinguish self from non-self, leading to subsequent secretion of specific cytokines[4,5] and receptor-mediated endocytosis of the glycosylated material.[6]

One well-studied example of an immune lectin is the mannose receptor (MR, CD206), also known as the macrophage mannose receptor.[7] This protein contains multiple domains with different binding specificities.[8] It has eight C-type lectin domains (CTLs) for which evidence suggests only one, CTL4, is active.[9] The other domains do seem to play a role in recognition of larger glycan structures, like yeast mannan.[10] The CTLs of the mannose receptor not only bind mannosides and oligomannosides, but also fucosides and N-acetyl-glucosamine-containing carbohydrates.[11]

In addition to the CTL-domain, the MR has two additional binding domains: a fibronectin type II domain, capable of binding collagen fragments,[12] and a cysteine-rich lectin domain (CRD) capable of binding to sulfated sugars, particularly 4-sulfo-N-acetyl-galactosamine and 3-sulfo-galactose containing oligosaccharides.[13]

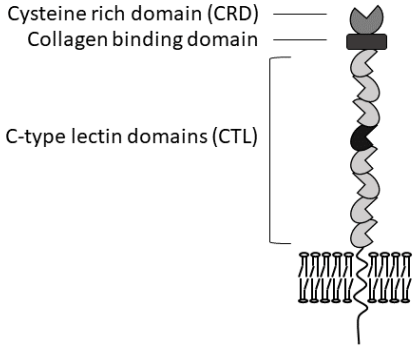

Figure 1. Cartoon representation of the mannose receptor (CD206). The CTL domain that is responsible for most of the calcium dependent oligosaccharide binding affinity (CTL4) is highlighted.

The biology of the MR is intriguing: it appears to enhance uptake of attached ligands in a receptor-dependent fashion, yet it possesses no internal signaling domains. In 2006, Kurts and co-workers[14] observed that MR-ligands showed enhanced antigen cross-presentation, while leaving MHC-II restricted antigen presentation unaffected. This effect seemed to be caused by differential routing of mannose receptor associated antigen compared to non-MR binding soluble antigen. As shown globally in Figure 2, regular pinocytosis of antigen targets an antigen to lysosomes, resulting in MHC class II presentation and activation of $CD4^+$ T-cells. MR-mediated uptake, however, results in sequestering of antigen in early endosomes, resulting in epitope presentation via MHC class I and activation of $CD8^+$ T-cells. This striking observation was deemed of importance to the field of vaccinology, as strong activation of a $CD8^+$ T-cell response is critical for anti-viral and anti-tumor vaccine regimes.[15] Achieving this using conventional vaccination strategies has proven difficult to date.[16]

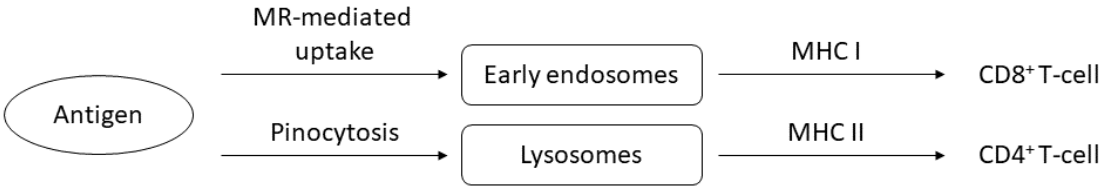

Figure 2. Simplified overview of the different routing of antigens and the different T-cell activations this results in, depending on MR-mediated uptake of antigen or uptake by pinocytosis.

Decoration of synthetic vaccines with MR-ligands is an area of active research.[17,18] Yet, to date, no direct correlation between mannoside-lectin binding characteristics and improved T-cell activation of a vaccine candidate has been made. This is largely due to the generally weak (mM to µM affinity) binding of carbohydrates to lectins.[11] This weak binding makes studying carbohydrate-lectin interactions using established techniques like surface plasmon resonance (SPR) or isothermal titration calorimetry (ITC) difficult. However, recently a microscopy-based method was developed that allowed for the evaluation of glycan-lectin interactions on the surface of a cell, using a points accumulation for imaging in nanoscale topography (PAINT) microscopy technique.

In PAINT microscopy, single molecule interactions are detected only when the fluorescent molecule under study is bound to some larger structure; the diffusional motion of unbound probe blurs the fluorescent signal to below detection limits. Interactions that slow the probe's diffusion for a certain length of time (hundreds of milliseconds), like glycan-lectin interactions, can be made visible as distinct events. The frequency these events are observed is correlated to the on-rate of the interaction, while the time (number of frames) they are visible is directly related to the off-rate. Glycoclusters were synthesized, containing various valences and configurations of carbohydrates, all containing a single fluorophore. By treating cells expressing the MR on the cell surface with low concentration (1-5 nM) of these probes, direct measurements of the lectin binding kinetics could be made for the first time. This method, dubbed "glyco-PAINT"[19] enables the direct, single molecule, observation of fluorescently labeled glycoclusters binding to the mannose receptor and the extraction of binding information from the approach.

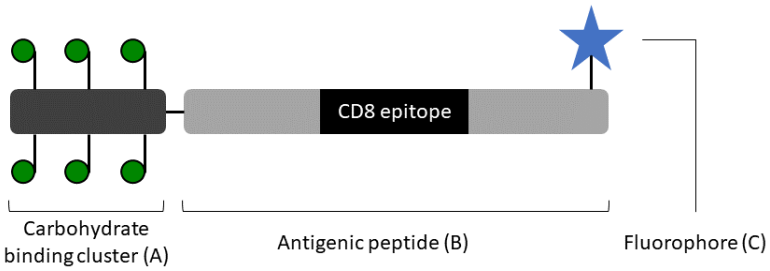

Figure 3. General design of the model antigenic peptides containing a mannose receptor binding carbohydrate cluster (A), an antigenic peptide containing a $CD8^+$ T-cell epitope (B) and a fluorophore (C) for tracking via glyco-PAINT.

It was envisaged that this technique could also be used to directly determine MR-binding kinetics of synthetic glycosylated vaccines. If this could then be combined with a $CD8^+$ T-cell activation study, a correlation between on-cell lectin binding kinetics and antigen cross-presentation could finally be established. This chapter describes the synthesis of a series of such glycosylated model peptides (Figure 3), containing a carbohydrate binding cluster (A, Figure 3), a CD8 T-cell epitope within flanking regions (B, Figure 3) and a fluorophore to allow glyco-PAINT of the constructs (C, Figure 3).

Results and Discussion

In order to study antigen uptake and cross-presentation using glyco-PAINT, a synthetic antigenic peptide bearing both one or more glycans as well as a fluorophore had to be designed and synthesized (Figure 4). As a first step in the design, the antigenic peptide was selected. The commonly employed model antigen $OVA_{247\text{-}264}$ was chosen as a first model antigen.[20,21] This peptide contains the MHC class I restricted epitope $OVA_{257\text{-}264}$ (SIINFEKL), commonly used in the study of antigen cross-presentation in mice and reagents for its immunological analysis are widely available. The $OVA_{247\text{-}264}$ peptide is often C-terminally extended with a A_5K spacer and previous work has indicated that the C-terminal lysine residue of this spacer can be modified with various functionalities without impairing antigen uptake and presentation.[21,22] This residue was therefore considered the preferred site for fluorophore introduction.

Similar previous work has also indicated that attachment of one or more azido-lysine residues N-terminal of the peptide is well tolerated in cross-presentation.[17,23] Propargylated glycans can then be installed by copper(I)-catalyzed azide alkyne cycloaddition (CuAAC). Variation of the number of azidolysines, as well as the spacing between the azidolysine residues enables the study of the effects multivalency has on the binding and internalization of glycosylated peptides. By introducing spacers of varying length between the azidolysine cluster and the N-terminus of the antigenic peptide, further optimization of the glycan-mediated uptake might be achieved. In the initial study, two spacers are compared: a single glycine residue and a triethylene-glycol based spacer, as described in Chapter 5. This last option could improve both aqueous solubility of the peptide as well as increasing the peptide's flexibility, and form an interesting contrast to the less flexible glycine spacer. Both of these spacer options are compatible with in-line Fmoc-SPPS, simplifying synthetic accessibility.

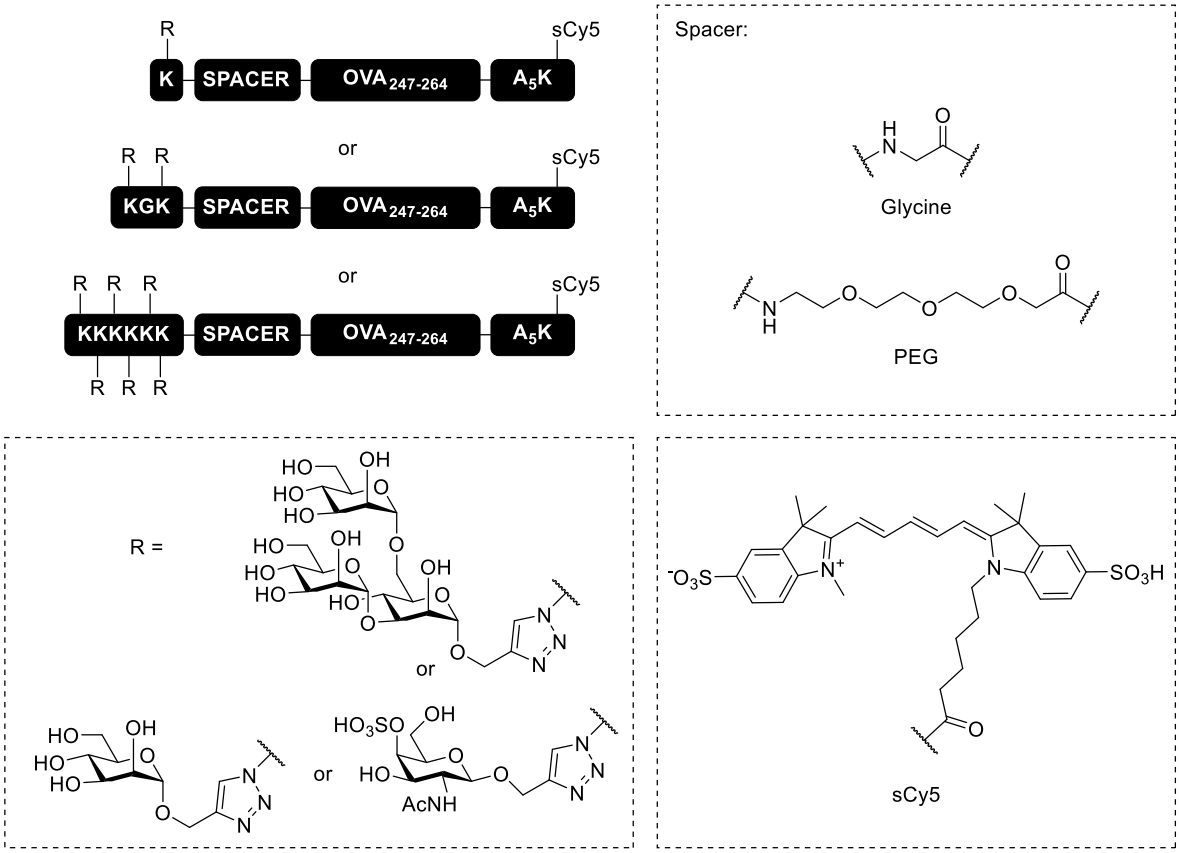

Figure 4. Overview of the proposed target peptides for the glyco-PAINT based studies on the correlation of mannose-receptor binding and CD8 T-cell cross-presentation. The $OVA_{247-264}$ peptide sequence contains the well-studied $OVA_{257-264}$ epitope, which is C-terminally extended with the amino acid sequence AAAAAK. This C-terminal lysine is then used for the introduction of the sulfoCy5 fluorophore. N-terminally an optional spacer can be introduced, followed by a cluster of one, two or six azidolysine residues conjugated with propargylated glycans via CuAAC chemistry.

Introduction of the propargylated glycans using CuAAC conjugation will be carried out as the last step, on the fluorescently labeled peptide scaffold (Figure 5A). The introduction of this fluorophore on the C-terminal lysine will be accomplished using on-resin coupling methods. To selectively modify this residue over the lysine residue that is present in the $OVA_{247-264}$ sequence, the C-terminal residue will be protected with the acid-labile monomethoxytrityl (Mmt) protective group, which can be liberated in a highly selective fashion. The synthesis of the fully protected, resin-bound antigenic peptide, containing the azidolysine residue required for carbohydrate conjugation, can be achieved using standard Fmoc-SPPS.

As the glycans of choice, mono- and trimannosides **1** and **2** (Figure 5B) were considered as good model mannosides to target the CTL domain of the mannose receptor, based on the data obtained in the original Glyco-PAINT experiments. These structures were previously shown to be on the lower and higher end of mannose receptor affinity respectively.[19] Furthermore, to target the CRD of the mannose receptor, a sulfated GalNAc derivative (**3**) was added to the library.[24,25] For the fluorophore, required to enable peptide tracking by Glyco-PAINT, the sulfo-

Cy5 dye (**4**) was selected. This dye is water soluble, super-resolution microscopy compatible,[26] and synthetically accessible.[27]

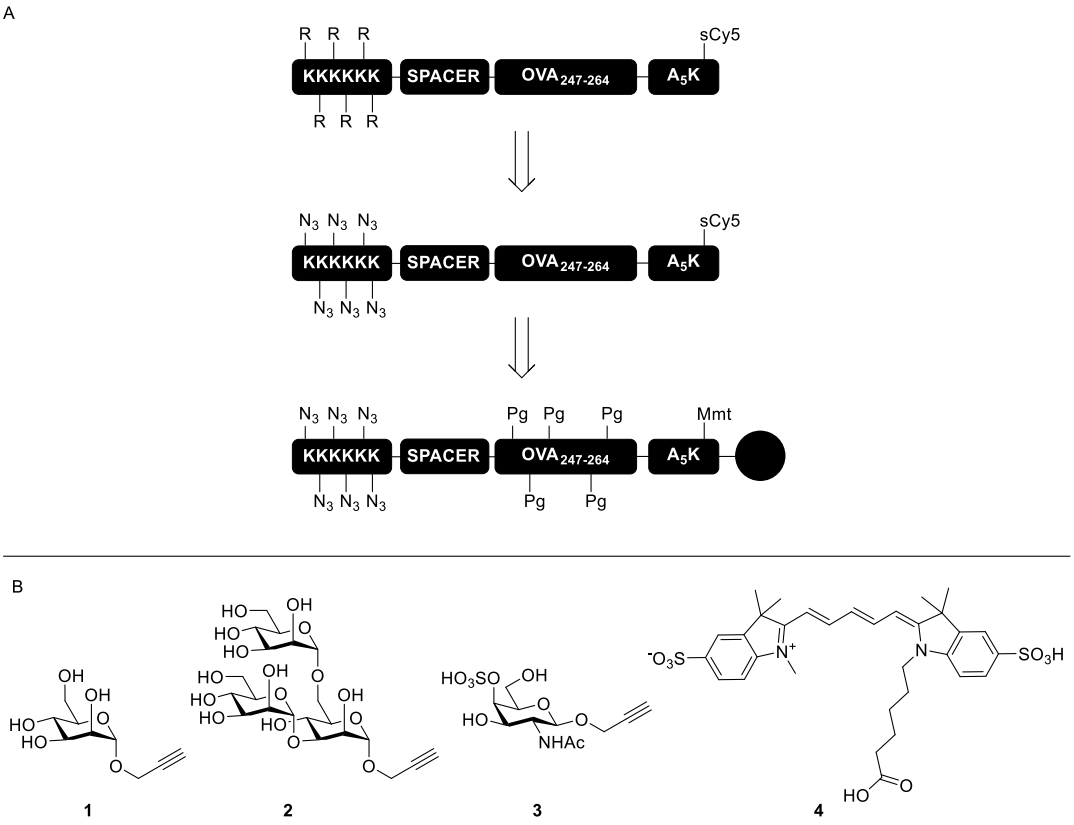

Figure 5. A) Retrosynthetic analysis of one of the target peptides. The R-groups represent different glycans linked via triazole-linkage, as in Figure 4. B) synthetic building blocks, required to furnish the differently glycosylated mannose receptor targeting fluorescent peptides.

To synthesize trimannoside **2**, a modified synthesis based on the work of Fairbanks and co-workers was explored.[28] In this work, this trimannoside was synthesized bearing a benzyl protecting group on the reducing end anomeric center. Replacing this with a propargyl group had no negative effect on the synthesis, as shown in Figure 6.

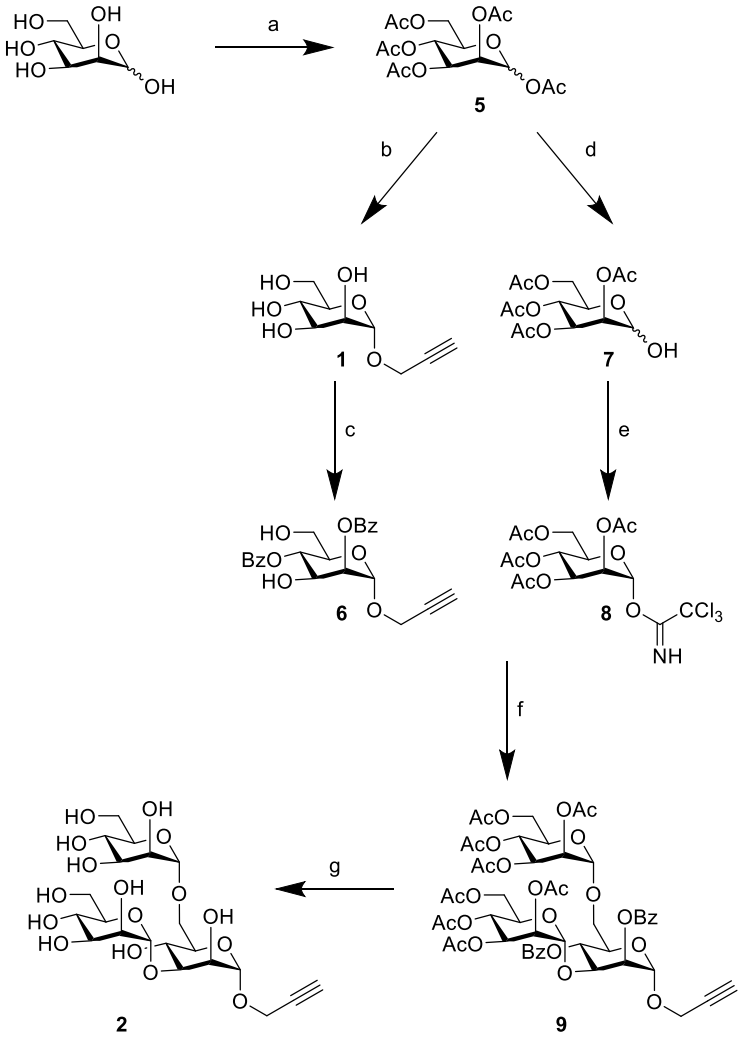

Figure 6. Synthesis of trimannoside **6**. Reagents and conditions: a) Ac_2O, pyridine, 93% b) i) Propargyl-OH, $BF_3{\cdot}Et_2O$, DCM, 63% ii) NaOMe, MeOH, 93% c) $Ph(OMe)_3$, TsOH, MECN ii) TFA, H_2O, 61% d) N,N-dimethylaminopropylamine, THF, 72% e) CCl_3CN, DBU, DCM, 70% f) $BF_3{\cdot}Et_2O$, 4Å molecular sieves, DCM, 62% g) Na(s), MeOH, 68%.

The first step of the synthesis was the acetylation of D-mannose to yield peracetylated sugar **5**. Propargyl alcohol was introduced at the anomeric position using $BF_3{\cdot}Et_2O$ as a catalyst, followed by Zemplén deacetylation with sodium methoxide in methanol to produce **1**. A portion of this sugar was reserved for later peptide conjugation. The bulk was regioselectively benzoylated on the 2- and 4-positions:[28,29] treatment of **1** with trimethylorthobenzoate and *para*-toluenesulfonic acid gave the 2,3:4,6-bis-orthoester intermediate, which can be hydrolyzed in the presence of TFA to give predominately the 2,4-benzoylated glycosyl acceptor **6**.

Intermediate **5** was also used to create lactol **7** using the selective anomeric deacetylation procedure reported by Andersen *et al.*[30] This intermediate was converted into trichloroacetimidate donor **8** using trichloroacetonitrile and catalytic DBU. The protected trisaccharide **9** was formed in 62% yield by reacting 4 equivalents of **8** with glycosyl acceptor

6, using $BF_3{\cdot}Et_2O$ as the activator. Deprotection of the ester groups under Zemplén conditions produced the propargyl-modified trimannoside **2**.

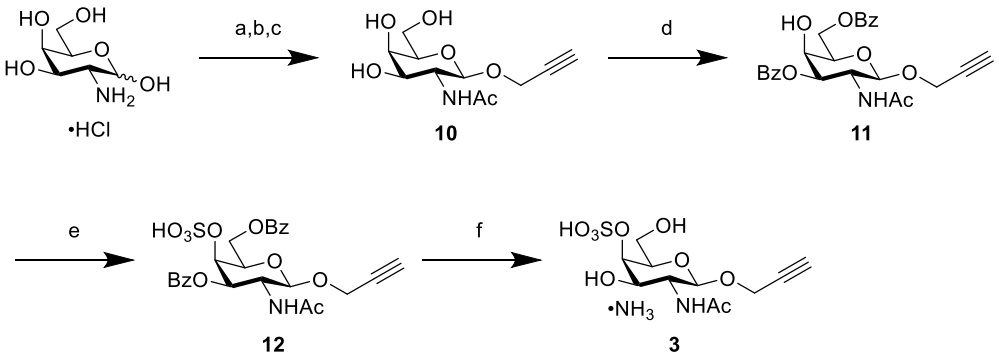

Figure 7. Synthesis of sulfated N-acetylgalactosamine derivative **3**. Reagents and conditions: a) Ac_2O, pyridine 84% b) propargyl-OH, $Yb(OTf)_3$ DCM, 94% c) NaOMe, MeOH, quant. d) BzCl, pyridine, DMF, -40°C, 55% e) $SO_3{\cdot}$pyridine, pyridine, 91% f) NH_3, H_2O, 75%.

The synthesis of the sulfated galactosamine derivative **3** began with the acetylation of D-galactosamine hydrochloride to yield peracetylated galactosamine in exclusively the β-configuration. The anomeric position was modified with propargyl alcohol using $Yb(OTf)_3$ as catalyst.[31] This was followed by deacetylation to produce propargylated *N*-acetylgalactosamine **10**. This intermediate was then benzoylated on the 3,6-positions. Initially, the conditions described by Imperiali and coworkers[32] were attempted, but the solubility of compound **10** in pyridine at -40°C was too low for the reaction to work efficiently. By dissolving the starting material in DMF, followed by cooling to -40°C and careful addition of benzoyl chloride in pyridine, the desired product **11** was obtained in 55% yield. This intermediate was sulfated using $SO_3{\cdot}$pyridine complex in 91% yield (**12**). Deacetylation using ammonium hydroxide produced the desired sulfated *N*-acetylgalactosamine **3**.

With the carbohydrate building blocks in hand, the focus was shifted to the synthesis of the fluorophore. The synthesis of such sulfated derivatives of cyanine dyes were originally described by Waggoner and coworkers.[27] To bring the structure in line with the commercially available cyanine dyes, a methyl substituent was placed on the indole nitrogen, instead of the ethyl used in the original publication (Figure 8).

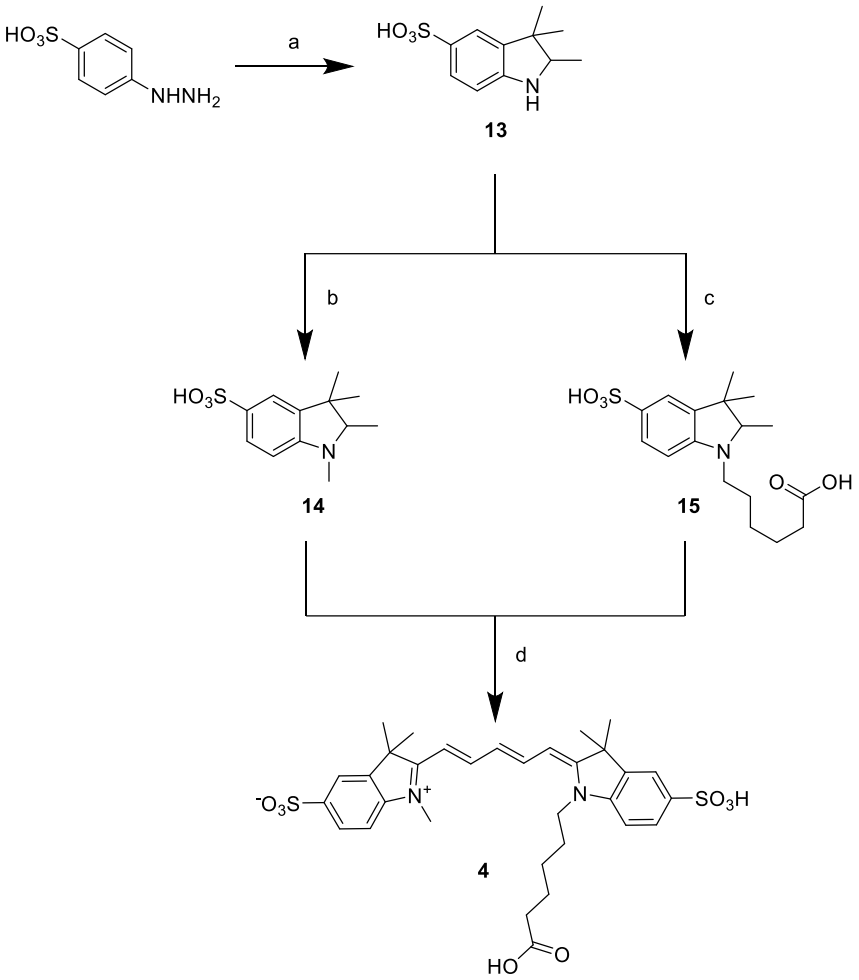

Figure 8. Synthesis of sulfoCy5 fluorophore **16**. Reagents and conditions: a) 3-methylbutanone, AcOH, 65% b) i) NaOAc, MeOH ii) MeI, MeCN, 80% c) i) KOAc, MeOH ii) 6-bromohexanoic acid, 1,2-dichlorobenzene, quant d) i) malonaldehyde bis(phenylimine) HCl, AcOH, Ac_2O, quant ii) Ac_2O, pyridine, 7%.

The synthesis of **4** started with a Fischer indole synthesis, yielding indoline **13** from *p*-hydrazinobenzenesulfonic acid and 3-methylketone. This indoline was alkylated with either iodomethane, producing **14**, or with 6-bromohexanoic acid, to produce **15.** To produce **4**, **14** was first reacted with an excess malonaldehyde bis(phenylimine), followed by a quick workup and further reaction with **15** to yield the asymmetric dye. Using RP-HPLC, the final product was obtained as the free carboxylic acid (**4**).

For the first attempt at a glycosylated and fluorophore labeled antigenic peptide, a simple monovalent design was endeavored (Figure 9). As a spacer moiety between the azidolysine residue and the antigenic peptide, a single glycine residue was introduced.

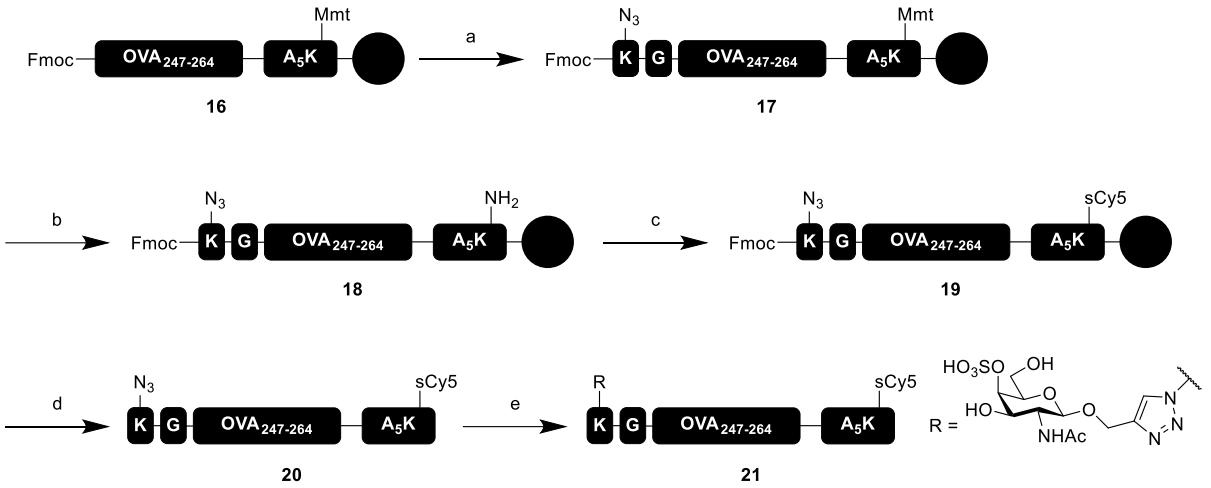

Figure 9. Synthesis of fluorescently labeled and glycosylated peptide **21**. Reagents and conditions: a) SPPS (2 cycles, HCTU, Fmoc-Gly-OH, Fmoc-Lys(N_3)-OH) b) i) AcOH, TFE, DCM ii) Et_3N, DMF c) **4**, HCTU, DiPEA, DMF d) i) 20% (v/v) piperidine/DMF ii) TFA, TIS, H_2O iii) RP-HPLC, 5.0 % e) **3**, $CuSO_4$, NaAsc, THPTA, 40°C, 74%.

The synthesis of resin bound peptide **16** was started by coupling of the Mmt-protected lysine onto Tentagel S RAM resin. Automated SPPS was then used to couple five alanine residues, followed by the native sequence of $OVA_{247-264}$. This peptide was then elongated with a glycine residue, followed by azidolysine, to yield resin bound peptide **17**. From this peptide, the Mmt-group was removed selectively using a mildly acetic mixture (1:2:7, AcOH/TFE/DCM)[33] followed by extensive washing with Et_3N in DMF to remove excess acetic acid. Fluorophore **4** was then coupled to the deprotected lysine sidechain using HCTU as a coupling agent. After coupling overnight, resin bound peptide **19** was obtained. Removal of the N-terminal Fmoc in **19** was followed by cleavage using a standard TFA deprotection mixture (95:2.5:2.5, TFA/TIS/H_2O) to yield a product mixture that, according to LC-MS analysis, contained product **20**, tainted with large quantities of a peptide with a mass spectrum indicating over-labeling with **4** (Δm = +624 Da), suggesting a second unprotected amine was present in (part of) resin bound peptide **18**. This could be caused by either unintentional cleavage of the Boc protecting group of the other lysine residue in the sequence, or by accidental partial cleavage of the Fmoc protecting group during the washing steps, with the latter being the most likely. The mixture was subjected to RP-HPLC and peptide **20** was isolated successfully in a yield of 5.0%. Next, conjugation of peptide **20** to the propargylated sulfosugar **3** under copper catalysis was attempted. Many different conditions for bioconjugation using copper catalysis have been described.[34,35] Initially, copper iodide was used as the source of Cu(I), with DiPEA and THPTA added to stabilize this reactive species, as was described previously for the synthesis of mannose glycoclusters.[19,36] However, this combination of reagents performed erratically, showing efficient conversion in some cases and no conversion in others. A different approach was taken instead: $CuSO_4$ was used as the copper source and was reduced *in situ* to Cu(I) using sodium ascorbate. The ligand THPTA[34] was added to stabilize the catalytically active species. The solvents were sparged with nitrogen before use, in order to remove dissolved oxygen that could potentially oxidize the Cu(I) species back to Cu(II). The purification of the product was

carried out using size exclusion chromatography with HW-40 resin[36], to remove the unreacted sugar, copper salts and small molecule ligands used in the reaction. The fluorophore present in the product allows for facile detection of product containing fractions via UV monitoring. This way, peptide **21** was obtained in a 74% yield.

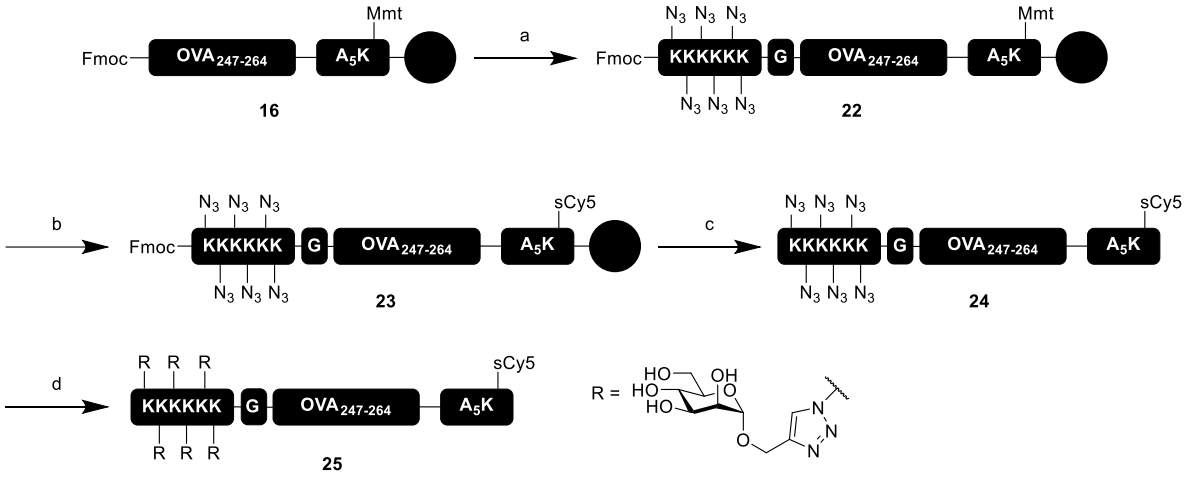

Figure 10. Synthesis hexaazide peptide scaffold **25**. Reagents and condition: a) SPPS (7 cycles, HCTU, Fmoc-Gly-OH, 6 x Fmoc-Lys(N_3)-OH) b) i) AcOH, TFE, DCM ii) Et_3N, DMF iii) **4**, HCTU, DiPEA, DMF c) i) 20% (v/v) piperidine/DMF ii) TFA, TIS, H_2O iii) RP-HPLC, 2.4% d) a) **1**, $CuSO_4$, NaAsc, THTPA, DMSO.

A peptide bearing 6 azidolysine residues was chosen as the next target as this would allow the comparison of MR-ligand valency on antigen cross-presentation. The synthesis of this peptide was started from resin bound peptide **16**, which was elongated with a single glycine residue, followed by six azidolysine residues to yield resin-bound intermediate **22**. The Mmt protecting group on **22** was cleaved under mild acidic conditions (AcOH/TFE/DCM, 1:2:7) followed by basic washes. Coupling of fluorophore **4** to the unmasked amine, mediated by HCTU, produced resin bound peptide **23**. Fmoc cleavage and global deprotection of the peptide using a TFA cocktail (95:2.5:2.5, TFA/TIS/H_2O) yielded crude **24**. This intermediate was again highly contaminated by large quantities of doubly labeled peptide. After RP-HPLC, pure **24** was obtained in 2.4% yield.

As, due to the low yields of SPPS, only limited quantities of **24** were available, the conjugation with propargyl mannoside **1** was attempted on a test-scale. Gratifyingly, the click reaction proceeded without incident, generating compound **25** cleanly based on LC-MS analysis (Figure 10). However, after purification over HW-40 size exclusion resin, some problems were encountered. The ammonium acetate used as buffer salt during the purification was not fully removable by lyophilization, even after repeated rounds of lyophilization. This, combined with the small scale of the reaction, meant the final yield of **25** could not be determined accurately. As the isolated yield of peptide **24** was rather poor, resynthesis using larger quantities of the peptide was not an immediate option. Therefore, improvements to the synthesis of the scaffold were considered a first priority.

To increase the yield of the fluorophore labeled scaffold peptide, the over-labeling problem in the fluorophore labeling step had to be eliminated. Since this problem is most likely caused by unintentional deprotection of the N-terminal Fmoc, acetylation of the N-terminus before fluorophore coupling was considered a viable strategy to explore.

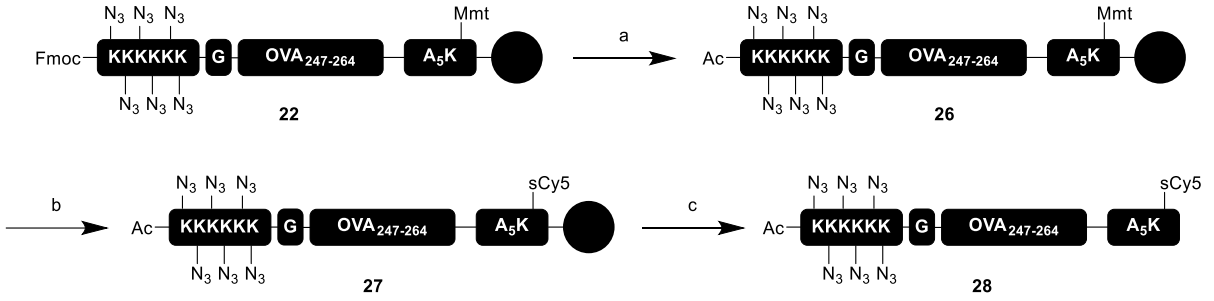

Figure 11. Synthesis of acetylated scaffold **29** from resin bound intermediate **23**. Reagents and conditions: a) i) 20 % (v/v) piperidine/DMF ii) Ac_2O, DiPEA, DMF b) i) AcOH, TFE, DCM ii) Et_3N, DMF iii) **4**, HCTU, DiPEA, DMF c) i) TFA, TIS, H_2O ii) RP-HPLC, 6.2%.

Previously synthesized intermediate **22** was N-terminally deprotected and acetylated by treating the resin bound peptide with a mixture of Ac_2O and DiPEA in DMF, producing resin bound peptide **26** (Figure 11). This peptide was then selectively deprotected and the fluorophore was introduced as before, producing **27**. After global deprotection of the peptide followed by RP-HPLC purification, **28** was obtained in 6.2% yield, a marked increase over the previous synthesis.

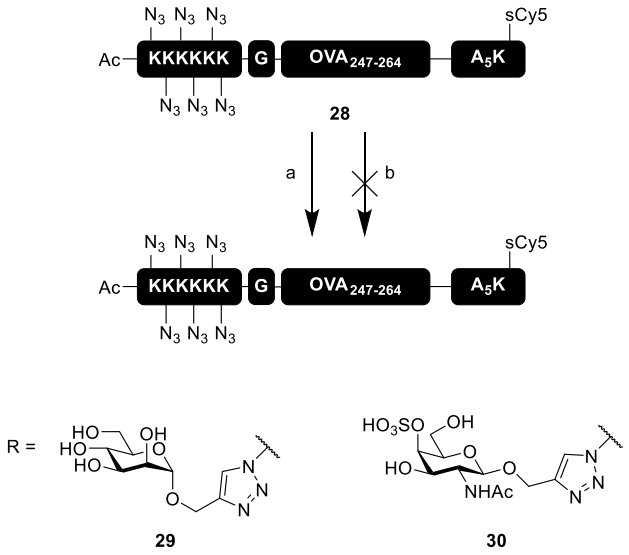

Figure 12. Conjugation of peptide scaffold **29** with mannoside **1** and attempted conjugation with sulfated glycoside **3**. Reagents and conditions: a) **1**, $CuSO_4$, NaAsc, THTPA, DMSO, 20% b) **3**, $CuSO_4$, NaAsc, THTPA, DMSO.

This peptide was again conjugated to monomannoside **1**. The solubility of the scaffold **28** was quite low even when using DMSO as main solvent, but conjugation with the mannoside did proceed to completion. During size exclusion chromatography over HW-40 resin, ammonium

bicarbonate was used as the buffer salt, which is easier to remove by lyophilization. This enabled the isolation of compound **29** in 20% yield. Next, an attempt was made to modify peptide **28** with sulfated glycan **3**. Unlike the modification with the neutrally charged mannoside, the Cu-catalyzed conjugation proceeded sluggishly for this sugar. LC-MS analysis after 72 hours of reaction time indicated the presence of a mixture of peptides, bearing various amounts of sugar **3**. The main component of the mixture had a mass-spectrum indicative of conjugation of only three sugars to the peptide. At the same time, the reaction mixture had started to turn gel-like, further indicating the low solubility of the scaffold as a problematic factor. After an additional 48 hours of reaction time, the complexity of the mixture had further increased and no products or intermediates could be identified by mass spectrometry analysis. Further dilution with DMSO or DMF could not redissolve the peptide, hindering thorough analysis and further conversion. At this point, the reaction was abandoned.

As these solubility issues were seriously hindering the synthesis of more complex peptides, the earlier described polyethyleneglycol spacer was considered as a replacement for the glycine spacer used up to now. This spacer should increase solubility in both organic and aqueous solvents, hopefully keeping the molecule in solution during the copper-catalyzed glycoconjugation. However, the length and flexibility of this moiety can also have considerable effect on the binding kinetics of the glycocluster, so direct comparison between peptides containing different spacers need to be considered carefully. The synthesis of a short PEG spacer compatible with Fmoc-SPPS will be described in Chapter 5, and this same spacer will be used here.

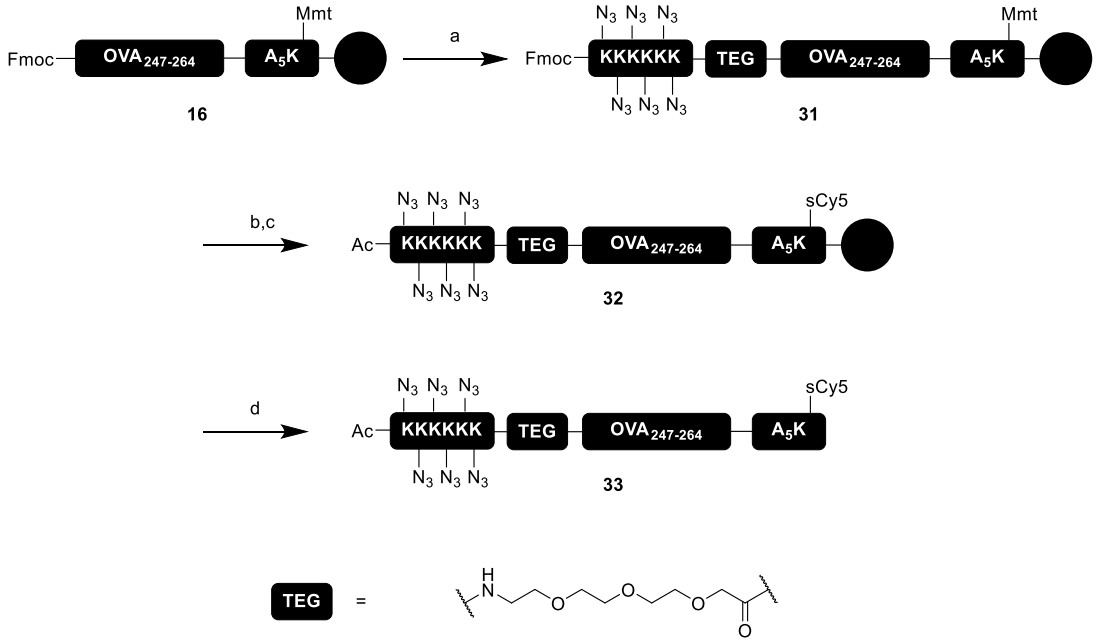

Figure 13. Synthesis of scaffold peptide **34** containing a polyethylene glycol spacer. Reagents and conditions: a) SPPS (7 cycles, HCTU, Fmoc-PEG-OH, 6 x Fmoc-Lys(N_3)-OH) b) i) 20 % (v/v) piperidine/DMF ii) Ac_2O, DiPEA, DMF c) i) AcOH, TFE, DCM ii) Et_3N, DMF iii) **4**, HCTU, DiPEA, DMF d) i) TFA, TIS, H_2O ii) RP-HPLC, 7.4%.

By extending resin bound peptide **16** with this PEG spacer, followed by elongation with six azidolysine residues, resin bound peptide **31** was obtained successfully. N-terminal acetylation followed by selective Mmt deprotection and HCTU mediated coupling of fluorophore **4** yielded resin bound peptide **32**. Global deprotection of this molecule followed by RP-HPLC purification yielded compound **33** in 7.4% yield. As expected, the solubility of this molecule was improved compared to the previously described compound **28**. Next, copper catalyzed click reactions with all three propargylated glycans were carried out on this scaffold.

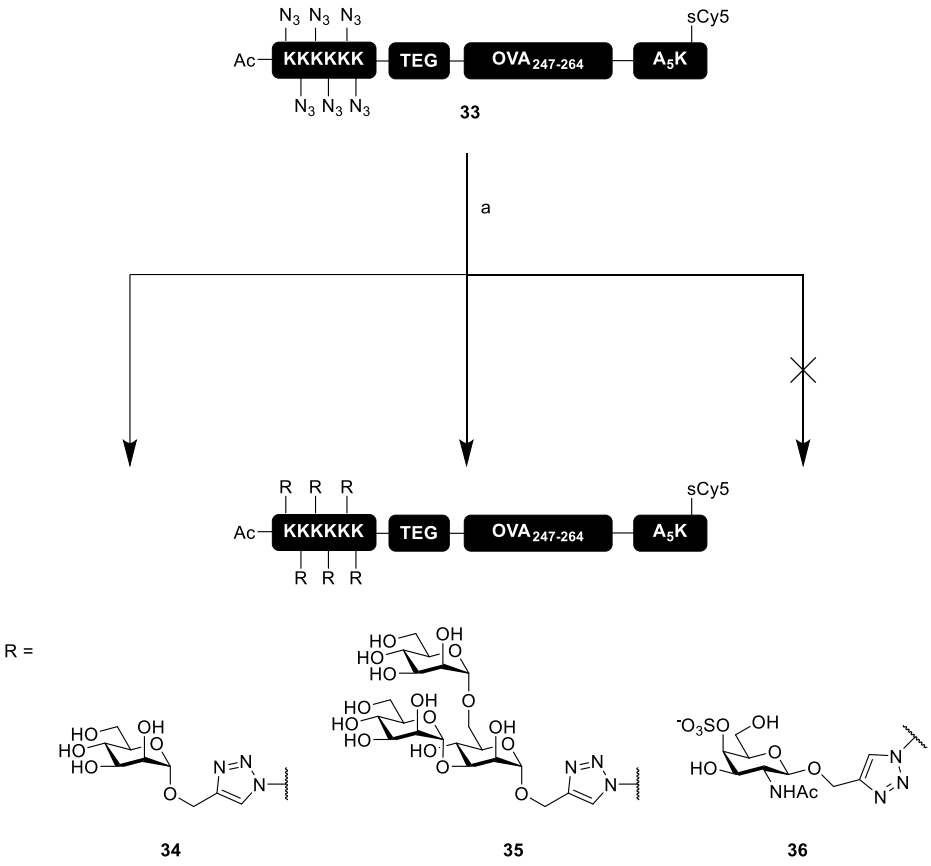

Figure 14. Synthesis of three different glycoconjugates based on scaffold **34**. Reagents and conditions: a) **1**, **2** or **3**, $CuSO_4$, NaAsc, THPTA, DMSO, 40°C, (**35:** 85%, **36:** 54%, **37:** -).

Conjugation of scaffold **33** with both the monomannoside **1** and trimannoside **2** worked without major issue in 85% and 54% yield respectively. The increase in yield observed for the hexa-monomannoside (compared to compound **29**) could indicate that the increase in solubility helps the reaction or the following purification. Sulfated glycan **3** was also subjected to copper catalyzed click with scaffold **33** in an attempt to produce conjugate **36**, and initially LC-MS analysis indicated formation of the desired glycopeptide from this reaction. An attempt was made to isolate this product using size exclusion chromatography, but after lyophilization of the main peak no product was observed by LC-MS analysis.

Since earlier work has found a correlation between multivalency and both lectin binding and cross-presentation, peptides with a different valency were explored next. Using the methods described above, synthesis of a peptide bearing two N-terminal azidolysine residues, with a glycine spacer between them, was carried out (Figure 15).

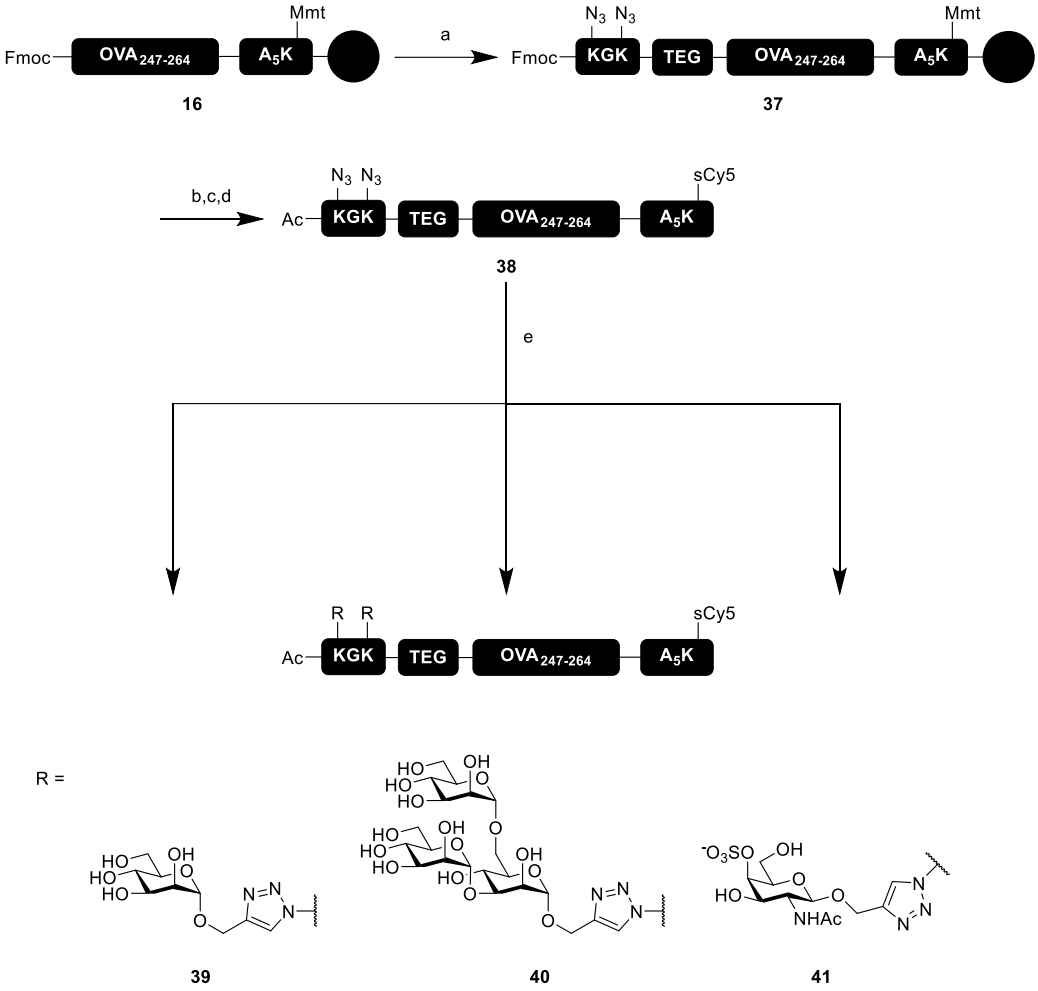

Figure 15. Synthesis of bivalent peptide scaffold **39** and glycoconjugates **40**, **41** and **42**. Reagents and conditions: a) SPPS (4 cycles, HCTU, Fmoc-PEG-OH, Fmoc-Lys(N_3)-OH, Fmoc-Gly-OH, Fmoc-Lys(N_3)-OH) b) i) 20 % (v/v) piperidine/DMF ii) Ac_2O, DiPEA, DMF c) i) AcOH, TFE, DCM ii) Et_3N, DMF iii) **4**, HCTU, DiPEA, DMF d) i) TFA, TIS, H_2O ii) RP-HPLC, 6.6% e) **1**, **2** or **3**, $CuSO_4$, NaAsc, THPTA, DMSO, 40°C, (**40:** 60%, **41:** 60%, **42:** 52%)**.**

Manual elongation of the resin bound peptide **16** with the TEG-spacer followed by Lys(N_3)-Gly-Lys(N_3) proceeded smoothly. This was followed by acetylation of the N-terminus, selective lysine deprotection and fluorophore incorporation. After global deprotection with TFA (95:2.5:2.5, TFA/TIS/H_2O) and RP-HPLC scaffold **38** was obtained in 6.6% yield. This scaffold was derivatized with all three propargylated glycans, producing all three bivalently glycosylated peptides in decent yields. Of particular note here is the fact that compound **41**, bearing two of the sulfo-GalNAc moieties was obtained without incident in fair yield. This indicates that the problems encountered while attempting to synthesize compounds **30** and **36** are most likely arriving from the amount of sulfated glycans introduced and are not an inherent problem of the sulfated glycan.

To evaluate whether the binding of these novel antigenic peptides could indeed be studied by glyco-PAINT, a binding density measurement was performed. In this experiment, the same mannose-receptor expressing Chinese hamster ovary (CHO) cells used for the original glyco-PAINT experiments were used.[19] Since CHO cells do not express any mannose-binding lectins by themselves, non-modified CHOs were used as negative controls. During the measurement, 1 nM of molecule **34** was added to the cells and a total of 5000 frames, with a 50 ms frame integration time, were recorded. Using the tracking software TrackMate[37] individual single-molecule binding events were detected as fluorescent puncta in the images. Next, using the tracking capability of the software, these individual binding events were linked together into tracks, effectively grouping together peptide-MR interactions that persisted over several frames. These tracks were converted to density maps by plotting the total amount of tracks per μm^2. These maps, together with the brightfield images of the cells, are shown in Figure 16.

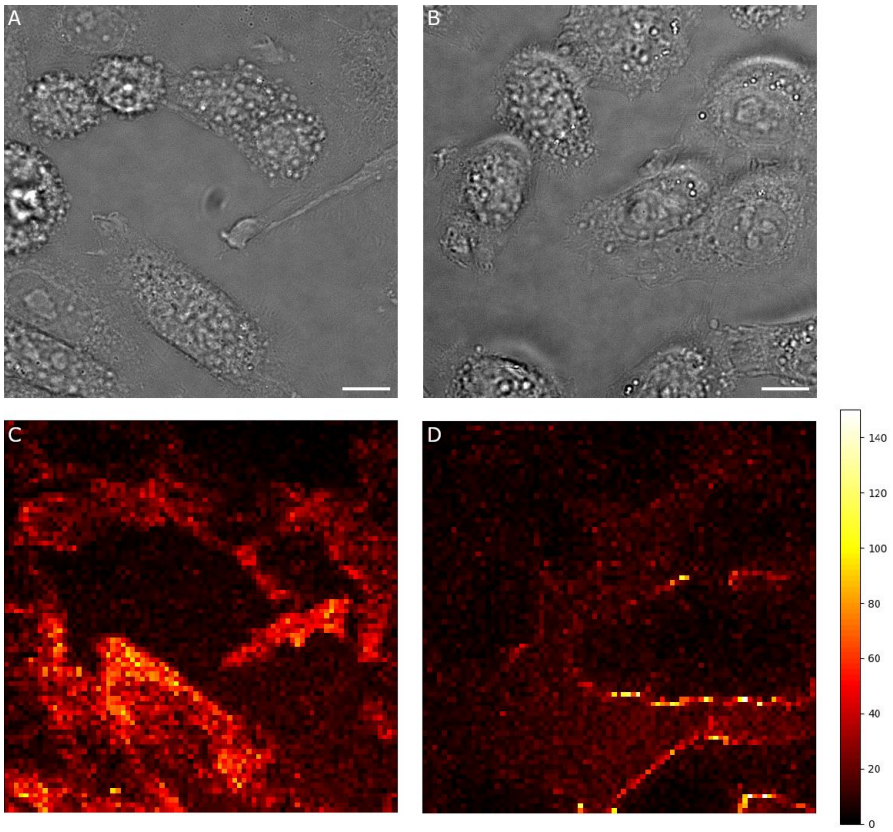

Figure 16. An example of glyco-PAINT used to determine binding affinity of glycosylated antigenic peptide **34**. Top half of figure: Brightfield images showing A) MR-transformed CHO and B) non-transfected wildtype CHO cells. Bottom half of figure: Density maps showing binding in events/μm^2 for C) MR-transformed CHO cells and D) non-transfected CHO cells. A single pixel in the density maps represents 1 μm^2 of cell area. The scale bar in brightfield images represents 10 µm.

In these maps, the difference in binding density between MR-expressing cells and the wild-type is apparent. This suggests that 1) the glycosylated antigenic peptides do indeed have binding interaction with the mannose receptor and 2) Glyco-PAINT can be used to measure the kinetics of this binding. In the near future, all glycosylated peptides described in this

chapter will be evaluated in this manner, and k_{off} and relative k_{on} values will be determined for all. Once these data are obtained, T-cell assays will be carried out using the different constructs to determine whether a correlation between one or more parameters of MR-binding and level of T-cell activation exist, using a dendritic cell mediated cross-presentation assay.

Conclusion

The effects glycosylation has on antigen (cross-)presentation are as of now not yet fully understood. Novel methods and tools to study lectin interaction, uptake and routing of, and T-cell activation by, glycosylated antigens are a key region of investigation. The glyco-PAINT method was developed to better measure the binding of glycans to lectins on a cell membrane, allowing for more accurate determination of some of the parameters involved in uptake of glycosylated antigen. Here, a series of glycosylated peptides were synthesized in an attempt to apply the glyco-PAINT methodology to glycosylated versions of the well-studied antigenic peptide $OVA_{247-264}$.

Incorporation of the required fluorophore was carried out by modification of the C-terminal A_5K modification. On-resin introduction of the fluorophore enabled facile conjugation of the fluorophore to the desired lysine residue, and the modified peptides were isolated in reasonable yields after RP-HPLC. For the introduction of the multivalent glycans, a strategy based on the introduction of a multivalent clickable scaffold, in the form of one or more azidolysine residues on the N-terminal side of the peptide, was utilized. These azide containing peptides can be modified with different propargylated glycans, creating diversity in both multivalency and glycan structure. Besides the already known propargyl mono- and trimannoside structures, a new novel sulfated GalNAc derivative, as a ligand for the cysteine rich domain of the mannose receptor, was developed.

During the synthesis of the larger scaffolds, some solubility problems were encountered. The solubility of the peptide was improved by the introduction of a PEG based spacer between the antigenic peptide and the poly-azidolysine scaffold. Using this improved scaffold, hexavalent peptides **34** and **35** could be synthesized successfully, as well as bivalent peptides **39**, **40** and **41**. Interestingly, both attempts to couple six sulfo-GalNAc molecules onto a hexavalent scaffold failed. Whether this is a problem caused by the high degree of sulfation, by negatively influencing either the click reaction or the following purification, remains to be investigated.

An initial glyco-PAINT experiment was carried out using peptide **34**, showing that this construct does indeed show MR-dependent binding interactions with cells. The technique will be further utilized to fully characterize the MR binding of molecules **34**,**35** and **39-41**.

Experimental

General methods for synthesis and characterization of compounds

Solvents were purchased from Honeywell, VWR or Alfa Aesar. Anhydrous solvents were prepared by drying over 4Å molecular sieves. Reagents purchased from chemical suppliers were used without further purification, unless stated otherwise. All reactions were performed under nitrogen atmosphere and/or under exclusion of H_2O, unless stated otherwise. Reactions were followed by thin layer chromatography which was performed using TLC silica gel 60 F254 on aluminium sheets, supplied by Merck. Compounds were visualized using UV absorption (254 nm) and/or a spray reagent, either permanganate (5 g/L $KMnO_4$, 25 g/L K_2CO_3) or sulfuric acid (10% v/v in EtOH). ^1H and ^{13}C NMR spectra were recorded using a Brüker AV400 (400 / 101 MHz) or a Brüker AV300 (300 / 75 MHz) and COSY and HSQC 2D experiments were used to assign peaks. Recorded data was interpreted and analyzed using MestReNova 12 software. Chemical shifts are reported in ppm (δ) in reference to an internal standard (TMS) or the residual solvent peak. High resolution mass spectra were recorded by direct injection (2 µL of a 2 µM solution in H_2O/MeCN 1:1 and 0.1% formic acid) on a mass spectrometer (Thermo Fisher Exactive HF Orbitrap) equipped with an electrospray ion source in positive mode. The high resolution mass spectrometer was calibrated prior to measurements with a calibration mixture (Thermo Finnigan). LC-MS characterization of compound was carried out using an electrospray ionization mass spectrometry (ESI-MS) on a Thermo Finnigan LCQ Advantage Max LC-MS instrument with a Surveyor PDA plus UV detector on an analytical C18 column (Phenomenex, 3 µm, 110 Å, 50 mm × 4.6 mm) in combination with buffers A (H_2O) and B (MeCN) containing a constant 10% C (1% aq TFA).

1,2,3,4,6-penta-O-acetate-D-mannopyranose (5)

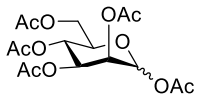

D-mannose (9.20 g, 50 mmol) was suspended in EtOAc (250 mL). Pyridine (10 eq., 40 mL, 500 mmol) and acetic anhydride (10 eq., 47 mL, 500 mmol) were added and the reaction was stirred overnight at room temperature. The reaction mixture was diluted with 250 ml EtOAc and washed once with 1M HCl (1 L) and twice with saturated $NaHCO_3$ (2 x 1 L) solution. The resulting organic layer was dried over $MgSO_4$, filtered and concentrated. Penta-acetyl mannose **5** was obtained as a viscous yellow oil (18.43 g, 47.2 mmol, 93%). The product was used in the next reaction steps without further purification. Spectral data was in accordance with earlier published results.[38]

Propargyl 2,3,4,6-tetra-O-acetyl-α-D-mannopyranoside (S1)

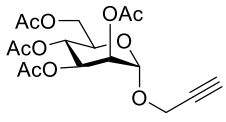

A solution of **5** (3.90 g, 10 mmol) in anhydrous DCM (50 mL) was cooled to 0°C in an ice bath. Propargyl alcohol (5 eq., 2.9 ml, 50 mmol) and $BF_3{\cdot}Et_2O$ (10 eq, 12.3 mL, 100 mmol) were added and the solution was warmed to room temperature. After 96 hours, the reaction was quenched by the addition of saturated aqueous $NaHCO_3$ (200 mL). The reaction mixture was further diluted by the addition of DCM (200 mL) and the organic layer was separated. The organic layer was washed once with saturated aqueous $NaHCO_3$ (200 mL) and twice with water. The organic layer was dried over $MgSO_4$, filtered and concentrated. Silica gel column chromatography (10→50% EtOAc in pentane) yielded **S1** as a colourless oil (2.43 g, 6.3 mmol, 63%). **^{1}H NMR** (300 MHz, $CDCl_3$) δ 5.36 – 5.26 (m, 3H, H2, H3, H4), 5.04 (d, *J* = 1.7 Hz, 1H, H1), 4.34 – 4.25 (m,

3H, H5, CH_2-propargyl), 4.12 (dd, *J* = 12.2, 2.5 Hz, 1H, H6a), 4.07 – 3.99 (m, 1H, H6b), 2.49 (t, *J* = 2.4 Hz, 1H, CH-propargyl), 2.17 (s, 3H, C(O)CH_3), 2.11 (s, 3H, C(O)CH_3), 2.05 (s, 3H, C(O)CH_3), 2.00 (s, 3H, C(O)CH_3). **^{13}C NMR** (75 MHz, $CDCl_3$) δ 170.8 (C=O), 170.1 (C=O), 170.0 (C=O), 169.8 (C=O), 96.3 (C1), 75.7 (CH-propargyl), 69.4 (C2), 69.1 (C5), 69.0 (C4), 66.1 (C3), 62.4 (C6), 55.1 (CH_2-propargyl), 21.0 (C(O)$\underline{C}H_3$), 20.9 (C(O)$\underline{C}H_3$), 20.8 (C(O)$\underline{C}H_3$).

Propargyl α-D-mannopyranoside (1)

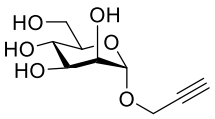

Acetylated glycoside **S1** (1.07 g, 2.76 mmol) was dissolved in MeOH (25 mL). a 30% (w/w) NaOMe in methanol solution (80 µL) was added and the reaction mixture was stirred for four hours. After TLC analysis indicated completion of the reaction, the reaction mixture was neutralized with Amberlyst H^+ resin. The resin was filtered off and the solution was concentrated *in vacuo*. Propargyl mannoside **1** was obtained as a crystalline white solid (0.56 g, 2.56 mmol, 93%). **^{1}H NMR** (300 MHz, MeOD) δ 4.96 (d, *J* = 1.7 Hz, 1H, H1), 4.27 (d, *J* = 2.4 Hz, 2H, CH_2-propargyl), 3.89 – 3.57 (m, 5H, H2, H3, H4, H6), 3.51 (ddd, *J* = 8.7, 5.8, 2.3 Hz, 1H, H5), 2.86 (t, *J* = 2.4 Hz, 1H, CH-propargyl). **^{13}C NMR** (75 MHz, MeOD) δ 99.8 (C1), 76.0 (CH propargyl), 75.0 (C5), 72.5 (C4), 72.0 (C2), 68.4 (C3), 62.8 (C6), 54.8 (CH_2-propargyl). **HRMS** (ESI) m/z: [M + Na^+] calcd for $C_9H_{14}O_6$ 241.0683, found 241.0681.

Propargyl 2,4-di-O-benzoyl-α-D-mannopyranoside (6)

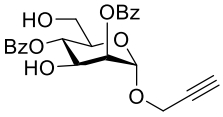

Glycoside **1** (0.53 g, 2.5 mmol) was dissolved in MECN (12.5 ml). Trimethyl orthobenzoate (2,5 eq., 1.1 ml, 6.2 mmol) and TsOH (0.1 eq., 48 mg, 0.25 mmol) were added and the solution was swirled until all solids were dissolved. The solution was stirred for another 5 minutes and the MECN was removed *in vacuo*. The obtained solid was redissolved in fresh MECN (5 ml) and 10% aqueous TFA (5 ml) was added. The solution was stirred for another 15 minutes and subsequently concentrated to dryness. The crude solid was purified by column chromatography (1:1 EtOAc:pentane) to obtain pure **6** as a white solid (0.65 g, 1.52 mmol, 61%). **^{1}H NMR** (300 MHz, $CDCl_3$) δ 8.13 – 8.03 (m, 4H, CH_{arom}), 7.65 – 7.56 (m, 2H, CH_{arom}), 7.51 – 7.41 (m, 4H CH_{arom}), 5.52 (t, *J* = 10.0 Hz, 1H, H4), 5.45 (dd, *J* = 3.5, 1.7 Hz, 1H, H2), 5.25 (d, *J* = 1.7 Hz, 1H, H1), 4.44 (dd, *J* = 10.0, 3.5 Hz, 1H, H3), 4.33 (d, *J* = 2.4 Hz, 2H, CH_2-propargyl), 4.00 (ddd, *J* = 10.0, 4.1, 2.4 Hz, 1H, H5), 3.86 – 3.70 (m, 2H, H6), 2.51 (t, *J* = 2.4 Hz, 1H, CH-propargyl). **^{13}C NMR** (75 MHz, $CDCl_3$) δ 167.4 (C=O), 166.1 (C=O), 133.9 (CH_{arom}), 133.8 (CH_{arom}), 130.1 (CH_{arom}), 129.3 (C_q), 129.1 (C_q), 128.8 (CH_{arom}), 128.7 (CH_{arom}), 96.7 (C1), 78.4 (C_q-propargyl) 75.6 (CH-propargyl), 72.8 (C2), 71.2 (C5), 70.3 (C4), 68.7 (C3), 61.5 (C6), 55.4 (CH_2-propargyl). **HRMS** (ESI) m/z: [M + Na^+] calcd for $C_{23}H_{22}O_8$ 449.1207, found: 449.1202.

2,3,4,6-tetra-O-acetyl-D-mannopyranose (7)

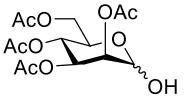

Anomeric deacetylation was carried out according to the procedure of Andersen et al.[30] Acetylated sugar **5** (9.93 g, 25 mmol) was dissolved in THF (125 mL). DMAPA (5 eq., 15.7 ml, 125 mmol) was added to the solution and the reaction mixture was stirred for 2 hours, after which TLC analysis indicated full consumption of starting material. The solution was transferred to a separation funnel and diluted with DCM (500 mL). The organic layer was washed successively with 1M HCl (500 mL) and brine (500 mL). The organic layer was dried over $MgSO_4$, filtered and concentrated producing the partially deacetylated sugar **7** (6.39 g, 18.3 mmol, 72%). This product was used in the next step without further purification. **^{1}H NMR** (300 MHz, $CDCl_3$) δ 5.42 (dd, J

= 10.0, 3.3 Hz, 1H, H3), 5.37 – 5.20 (m, 3H, H1, H2, H4), 4.62 (d, J = 4.2 Hz, 1H, 1-OH), 4.32 – 4.21 (m, 2H, H5, H6a), 4.19 – 4.09 (m, 1H, H6b), 2.17 (s, 3H, C(O)CH_3), 2.11 (s, 3H, C(O)CH_3), 2.06 (s, 3H, C(O)CH_3), 2.01 (s, 3H, C(O)CH_3). **^{13}C NMR** (75 MHz, $CDCl_3$) δ 171.0 (C=O), 170.4 (C=O), 170.2 (C=O), 170.0 (C=O), 92.1 (C1), 70.3 (C2), 68.9 (C3), 68.3 (C5), 66.3 (C4), 62.7 (C6), 20.9 (C(O)$\underline{C}H_3$), 20.8 (C(O)$\underline{C}H_3$), 20.8 (C(O)$\underline{C}H_3$).

Trichloroacetimidate 2,3,4,6-tetra-O-acetyl-D-mannopyranoside (8)

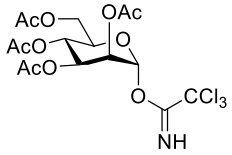

Partially protected compound **7** (1.74 g, 5.0 mmol) was co-evaporated three times with toluene. The flask was backfilled with N_2 and the sugar was dissolved in anhydrous DCM (25 mL). Trichloroacetonitrile (5 eq., 2.5 ml, 25 mmol) and DBU (0.1 eq., 77 mg, 0.5 mmol) were added and the reaction was allowed to stir at room temperature for 2.5 hours. Celite was added to the reaction and the volatiles were removed *in vacuo*. Silica gel column chromatography on neutralized silical (1:1 Et_2O:pentane) yielded trichloroacetimidate **8** a colorless solid (1.64 g, 3.34 mmol, 70%). **^{1}H NMR** (300 MHz, $CDCl_3$) δ 8.80 (s, 1H, C(NH)CCl_3), 6.29 (d, *J* = 1.9 Hz, 1H, H1), 5.50 – 5.39 (m, 3H, H2, H3, H4), 4.32 – 4.24 (m, 1H, H6a), 4.24 – 4.13 (m, 2H, H5, H6b), 2.21 (s, 3H, C(O)CH_3), 2.09 (s, 3H, C(O)CH_3), 2.07 (s, 3H, C(O)CH_3), 2.01 (s, 3H, C(O)CH_3). **^{13}C NMR** (75 MHz, $CDCl_3$) δ 170.0 (C=O), 169.9 (C=O), 169.9 (C=O), 169.7 (C=O), 159.9 ($\underline{C}$(NH)CCl_3), 94.6 (C1), 71.3 (C5), 68.9 (C2) , 68.0 (C3), 65.5 (C4), 62.2 (C6), 20.9 (C(O)$\underline{C}H_3$), 20.8 (C(O)$\underline{C}H_3$), 20.8 (C(O)$\underline{C}H_3$), 20.7 (C(O)$\underline{C}H_3$).

Propargyl 2,3,4,6-tetra-O-acetyl-α-D-mannopyranosyl-(1→6)-[2,3,4,6-tetra-O-acetyl-α-D-mannopyranosyl-(1→3)]-2,4-di-O-benzoyl-α-D-mannopyranoside (9)

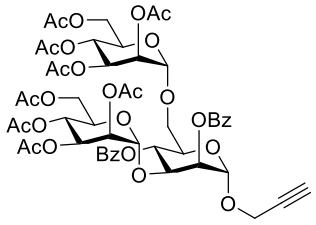

Glycosyl acceptor **6** (0.21 g, 0.5 mmol) was co-evaporated 3 times with toluene and dissolved in anhydrous DCM (25 mL) under an N_2 atmosphere. In a separate dry flask imidate donor **8** (4 eq., 0.99 g, 2.0 mmol) was dissolved in anhydrous DCM (5 mL). The solution containing the imidate was transferred to the reaction flask with a syringe and activated 4Å molecular sieves (1.26 g) were added. After stirring for one hour $BF_3{\cdot}Et_2O$ (2 eq, 0.12 ml, 1.0 mmol) was added and the solution was stirred overnight. The reaction was quenched by adding Et_3N (20 eq., 2.8 mL). The reaction mixture was filtered over celite and water (150 mL) was added. The layers were separated and the aqueous layer extracted twice with DCM (2 x 50 mL). The organic fractions were combined, dried and concentrated. The crude compound was purified by silica gel column chromatography (30% EtOAc in DCM) to produce pure **9** as a colorless solid (0.34 g, 0.31 mmol, 62%). **^{1}H NMR** (400 MHz, $CDCl_3$) δ 8.18 – 8.13 (m, 2H, CH_{arom}), 8.06 – 8.01 (m, 2H, CH_{arom}), 7.67 – 7.52 (m, 4H, CH_{arom}), 7.49 – 7.43 (m, 2H, CH_{arom}), 5.65 (t, *J* = 10.0 Hz, 1H), 5.55 (dd, *J* = 3.4, 1.8 Hz, 1H), 5.34 (dd, *J* = 10.1, 3.4 Hz, 1H), 5.29 – 5.20 (m, 3H), 5.11 – 5.06 (m, 2H), 4.98 (d, *J* = 1.9 Hz, 1H), 4.88 (dd, *J* = 2.9, 1.8 Hz, 1H), 4.81 (d, *J* = 1.7 Hz, 1H), 4.49 (dd, *J* = 9.8, 3.4 Hz, 1H), 4.37 (d, *J* = 2.4 Hz, 2H, CH_2-propargyl), 4.25 – 3.97 (m, 8H), 3.91 (dd, *J* = 10.8, 6.7 Hz, 1H), 3.62 (dd, *J* = 10.8, 2.2 Hz, 1H), 2.56 (t, *J* = 2.4 Hz, 1H, CH-propargyl), 2.14 (s, 3H, C(O)CH_3), 2.12 (s, 3H, C(O)CH_3), 2.05 (s, 3H, C(O)CH_3), 1.99 (s, 3H, C(O)CH_3), 1.95 (s, 3H, C(O)CH_3), 1.94 (s, 3H, C(O)CH_3), 1.85 (s, 3H, C(O)CH_3), 1.83 (s, 3H, C(O)CH_3). **^{13}C NMR** (101 MHz, $CDCl_3$) δ 170.8 (C=O), 170.7 (C=O), 170.1 (C=O), 169.9 (C=O), 169.8 (C=O), 169.2 (C=O), 166.0 (C=O), 165.4 (C=O), 133.8 (CH_{arom}), 133.7 (CH_{arom}), 130.1 (CH_{arom}), 130.0 (CH_{arom}), 129.2 (C_q), 128.9 (CH_{arom}), 128.8 (C_q), 128.7 (CH_{arom}), 99.5, 97.3, 96.2, 78.1 (C_q-propargyl), 75.8 (CH-propargyl), 75.0, 71.6, 70.1, 69.4, 69.3, 69.1, 68.8, 68.7, 68.4, 66.8, 66.1, 65.9, 62.5, 62.4, 55.1 (CH_2-propargyl),

21.0 (C(O)$\underline{C}H_3$), 20.9 (C(O)$\underline{C}H_3$), 20.8 (C(O)$\underline{C}H_3$), 20.7 (C(O)$\underline{C}H_3$), 20.5 (C(O)$\underline{C}H_3$). **HRMS** (ESI) m/z: [M + NH_4^+] calcd for $C_{51}H_{58}O_{26}$ 1104.3555, found 1104.3553

Propargyl α-D-mannopyranosyl-(1→6)-[α-D-mannopyranosyl-(1→3)]-α-D-mannopyranoside (2)

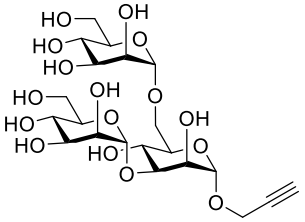

A small amount of sodium metal was dissolved in 5 ml MeOH (pH > 12). The methoxide solution was added to a flask containing **9** (0.32 g, 0.29 mmol) and the solution was stirred for 6 days. The reaction mixture was acidified with Amberlyst H+ and filtered. The solution was concentrated to dryness and the product was redissolved in 2 ml MeOH. The product was precipitated from 30 ml ice-cold diethyl ether. The ether was removed via centrifugation and the solids were washed with fresh Et_2O. The product was dried under vacuum yielding pure **2** as a white powder (0.12 g, 0.22 mmol, 68%). The obtained spectral data was consistent to earlier published results.[39] **^{1}H NMR** (400 MHz, MeOD) δ 5.06 (d, *J* = 1.4 Hz, 1H), 4.84 (d, *J* = 1.5 Hz, 1H), 4.26 (t, *J* = 2.1 Hz, 2H, CH_2-propargyl), 4.04 (dd, *J* = 3.0, 1.8 Hz, 1H), 4.00 – 3.90 (m, 2H), 3.89 – 3.58 (m, 18H), 2.89 (t, *J* = 2.4 Hz, 1H, CH-propargyl). **^{13}C NMR** (101 MHz, MeOD) δ 104.0, 101.5, 100.2, 80.7, 76.1 (CH-propargyl), 74.9, 74.4, 73.8, 72.6, 72.4, 72.1, 72.1, 71.2, 68.7, 68.5, 67.3, 67.1, 62.8, 55.0 (CH_2-propargyl). **HRMS** (ESI) m/z: [M + NH_4^+] calcd for $C_{21}H_{34}O_{16}$ 560.2185, found 560.2189

1,3,4,5-tetra-O-acetyl-2-deoxy-2-acetamido-β-D-galactopyranoside (S2)

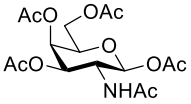

This reaction was carried out as described by Wipf et al.[40] Galactosamine hydrochloride (2.16 g, 10 mmol) was suspended in anhydrous pyridine (20 mL) and acetic anhydride (12 eq, 11.3 mL, 120 mmol) was added. The reaction was stirred overnight and decanted into ice cold water (200 mL). The precipitate was collected by filtration and dried in vacuo, yielding the title compound **S2** (3.25 g, 8.4 mmol, 84%) as a white solid. Traces of water were removed by co-evaporation with toluene. **^{1}H NMR** (400 MHz, $CDCl_3$) δ 5.70 (d, J = 8.8 Hz, 1H, H1), 5.45 (d, J = 9.6 Hz, 1H, NH), 5.38 (dd, J = 3.4, 1.2 Hz, 1H, H4), 5.09 (dd, J = 11.3, 3.3 Hz, 1H, H3), 4.45 (dt, J = 11.4, 9.2 Hz, 1H, H2), 4.21 – 4.07 (m, 2H, H6), 4.03 (td, J = 6.5, 1.2 Hz, 1H, H5), 2.18 (s, 3H, C(O)CH_3), 2.14 (s, 3H, C(O)CH_3), 2.05 (s, 3H, C(O)CH_3), 2.03 (s, 3H, C(O)CH_3), 1.95 (s, 3H, C(O)CH_3). **^{13}C NMR** (101 MHz, $CDCl_3$) δ 170.9 (C=O), 170.6 (C=O), 170.4 (C=O), 170.3 (C=O), 169.7 (C=O), 93.2 (C1), 72.0 (C5), 70.4 (C3), 66.5 (C4), 61.4 (C6), 50.0 (C2), 23.5 (C(O)$\underline{C}H_3$), 21.0 (C(O)$\underline{C}H_3$), 20.8 (C(O)$\underline{C}H_3$), 20.8 (C(O)$\underline{C}H_3$).

Propargyl 3,4,5-tri-O-acetyl-2-deoxy-2-acetamido-β-D-galactopyranoside (S3)

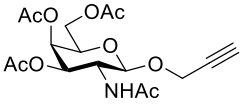

Compound **S2** (778 mg, 2 mmol) was suspended in anhydrous DCM (10 mL). Propargyl alcohol (10 eq, 1.15 mL, 20 mmol) and $Yb(OTf)_3$ (5 mol%, 62 mg) were added. The mixture was refluxed overnight. TLC analysis (100% EtOAc) indicated complete consumption of starting material and the reaction was allowed to cool to room temperature. The reaction mixture was further diluted with DCM and washed once with H_2O. The organic layer was dried over $MgSO_4$ and concentrated under reduced pressure. Silica gel column chromatography (4/1 EtOAc/pentane → 100% EtOAc) yielded compound **S3** as a white solid (569 mg, 1.88 mmol, 94%). **^{1}H NMR** (400 MHz, $CDCl_3$) δ 6.12 (d, J = 8.8 Hz, 1H, NH), 5.38 (d, J = 2.9 Hz, 1H, H4), 5.32 (dd, J = 11.2, 3.4 Hz, 1H, H3), 4.90 (d, J = 8.4 Hz, 1H, H1), 4.40 (d, J = 2.3 Hz, 2H, CH2-propargyl), 4.21 – 3.96 (m, 4H, H6, H2, H5), 2.51 (t, J = 2.3 Hz, 1H, CH-propargyl), 2.16 (s, 3H, C(O)CH_3), 2.06 (s, 3H, C(O)CH_3), 2.01 (s, 3H,

C(O)CH_3), 1.98 (s, 3H, C(O)CH_3). **^{13}C NMR** (101 MHz, $CDCl_3$) δ 170.8 (C=O), 170.5 (C=O), 170.4 (C=O), 98.7 (C1), 78.7 (Cq-propargyl), 75.4 (CH-propargyl), 70.8 (C5), 70.0 (C3), 66.8 (C4), 61.5 (C6), 55.9 (CH_2-propargyl), 51.0 (C2), 23.5 (C(O)$\underline{C}H_3$), 20.7 (C(O)$\underline{C}H_3$).

Propargyl 2-deoxy-2-acetamido-β-D-galactopyranoside (10)

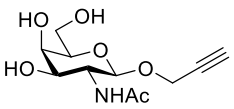

Compound **S3** (555 mg, 1.83 mmol) was dissolved in MeOH (18 mL) and a catalytic amount of metallic sodium was added. After 2 h, TLC (10% MeOH in EtOAc) indicated full consumption of starting material. The reaction was quenched by the addition of Amberlite® H+ resin and filtered. The volatiles were removed under reduced pressure and **10** was obtained in quantitative yield as a white solid. **^{1}H NMR** (400 MHz, MeOD) δ 4.57 (d, J = 8.4 Hz, 1H, H1), 4.37 (dd, J = 2.4, 1.0 Hz, 2H, CH2-propargyl), 3.93 (dd, J = 10.7, 8.4 Hz, 1H, H2), 3.84 (dd, J = 3.4, 1.0 Hz, 1H, H4), 3.78 (dd, J = 11.4, 7.0 Hz, 1H, H6a), 3.73 (dd, J = 11.4, 5.2 Hz, 1H, H6b), 3.63 (dd, J = 10.7, 3.3 Hz, 1H, H3), 3.51 (ddd, J = 6.8, 5.2, 1.1 Hz, 1H, H5), 2.85 (t, J = 2.4 Hz, 1H, CH-propargyl), 1.99 (s, 3H, NHC(O)C$\underline{H}_3$). **^{13}C NMR** (101 MHz, MeOD) δ 100.8 (C1), 80.1 (Cq-propargyl), 76.9 (C5), 76.0 (CH-propargyl), 73.1 (C3), 69.6 (C4), 62.5 (C6), 56.3 (CH_2-propargyl), 54.0 (C2), 23.0 (NHC(O)$\underline{C}H_3$).

Propargyl 3,6-di-O-benzoyl-2-deoxy-2-acetamido-β-D-galactopyranoside (11)

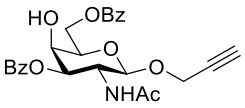

Deprotected sugar **10** (470 mg, 1.8 mmol) was co-evaporated with toluene (3x) and dissolved in anhydrous DMF (3.6 mL). The reaction mixture was cooled to -40°C before a solution of benzoyl chloride (2.2 eq, 465 µL, 3.96 mmol) in anhydrous pyridine (1.8 mL) was added dropwise. The reaction mixture was kept at -40°C for 1 h before allowing it to warm to room temperature. The reaction was stirred an additional 20 h, when TLC (70% EtOAc in pentane) indicated complete consumption of starting material. The reaction mixture was concentrated under reduced pressure and subjected to silica gel column chromatography (1/1 EtOAc/pentane → 9/1 EtOAc/pentane). This yielded the title compound **11** as a white solid (469 mg, 1.0 mmol, 55%). **^{1}H NMR** (400 MHz, MeOD) δ 8.10 – 8.01 (m, 4H, CH_{arom}), 7.66 – 7.56 (m, 2H, CH_{arom}), 7.53 – 7.42 (m, 4H, CH_{arom}), 5.19 (dd, J = 11.1, 3.2 Hz, 1H, H3), 4.60 (dd, J = 11.3, 7.4 Hz, 1H, H6a), 4.55 – 4.44 (m, 2H, H6b, H2), 4.43 – 4.34 (m, 2H, CH_2-propargyl), 4.28 (dd, J = 3.3, 1.1 Hz, 1H, H4), 4.08 (ddd, J = 7.4, 5.2, 1.1 Hz, 1H, H5), 2.87 (t, J = 2.4 Hz, 1H, CH-propargyl), 1.87 (s, 3H, NHC(O)C$\underline{H}_3$). **^{13}C NMR** (101 MHz, MeOD) δ 173.6 (C=O), 167.7 (C=O), 167.5 (C=O), 134.5 (CH_{arom}), 134.4 (CH_{arom}), 131.2 (C_q), 131.1 (C_q), 130.9 (CH_{arom}), 130.6 (CH_{arom}), 129.6 (CH_{arom}), 129.6 (CH_{arom}), 100.4 (C1), 79.7 (C_q-propargyl), 76.5 (CH-propargyl), 75.7 (C3), 74.0 (C5), 67.2 (C4), 64.8 (C6), 56.4 (CH_2-propargyl), 51.2 (C2), 22.8 (NHC(O)$\underline{C}H_3$).

Propargyl 3,6-di-O-benzoyl-4-O-sulfo-2-deoxy-2-acetamido-β-D-galactopyranoside (12)

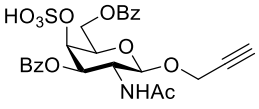

Compound **11** (65 mg, 0.14 mmol) was dissolved in anhydrous pyridine (2.8 mL) and SO_3·pyridine complex (5 eq, 111 mg, 0.7 mmol) was added and the reaction was heated to 50°C. After 1.5 h, TLC (100% EtOAc) indicated full consumption of starting material. The reaction was allowed to cool to room temperature, after which the mixture was concentrated under reduced pressure. Silica gel column chromatography (EtOAc → 1/4 MeOH/EtOAc) yielded the title compound **12** (70 mg, 128 µmol, 91%) as a white solid. **^{1}H NMR** (400 MHz, MeOD) δ 8.17 – 8.00 (m, 4H, Bz), 7.63 – 7.52 (m, 2H, Bz), 7.51 – 7.40 (m, 4H, Bz), 5.31 (dd, J = 11.2, 3.3 Hz, 1H, H3), 5.04 (d, J = 3.2 Hz, 1H, H4), 4.67 (d, J = 6.5 Hz, 2H, H6), 4.43 – 4.31 (m, 3H, H2,

CH2-propargyl), 4.17 (td, J = 6.1, 5.7, 0.9 Hz, 1H, H5), 2.85 (t, J = 2.4 Hz, 1H, CH-propargyl), 1.87 (s, 3H, C(O)CH_3). **^{13}C NMR** (101 MHz, MeOD) δ 167.8 (C=O), 134.3 (CH_{arom}), 134.0 (CH_{arom}), 131.4 (C_q), 131.4 (C_q), 131.1 (CH_{arom}), 130.7 (CH_{arom}), 129.5 (CH_{arom}), 129.3 (CH_{arom}), 100.2 (C1), 79.5 (Cq-propargyl), 76.6 (CH-propargyl), 73.7 (C5), 73.3 (C3), 73.2 (C4), 65.4 (C6), 56.4 (CH2-propargyl), 51.6 (C2), 22.8 (C(O)$\underline{C}H_3$). **HRMS** (ESI) m/z: [M + Na^+] calcd $C_{25}H_{25}NO_{11}S$ 570.1041, found 570.1042

Propargyl 4-O-sulfo-2-deoxy-2-acetamido-β-D-galactopyranoside ammonium salt (3)

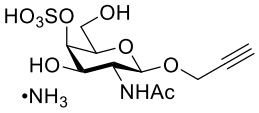

Compound **12** (90 mg, 0.16 mmol) was suspended in 28% aqueous ammonia (1.6 mL) and stirred at RT for 24h, at which time TLC (20% MeOH in EtOAc) indicated complete consumption of starting material. The reaction mixture was then diluted with water and washed with diethyl ether (3x). The organic layer was discarded and the aqueous layer concentrated under reduced pressure. The obtained residue was subjected to silica gel column chromatography (EtOAc → 1/1 MeOH/EtOAc) and the purified product was lyophilized to yield the title compound **3** as a with powder (42 mg, 0.12 mmol, 75%). **^{1}H NMR** (400 MHz, D_2O) δ 4.72 – 4.68 (m, 1H, H1), 4.66 (d, J = 2.1 Hz, 1H, H4), 4.39 (t, J = 2.4 Hz, 2H, CH_2-propargyl), 3.91 – 3.84 (m, 2H, H3, H2), 3.82 – 3.76 (m, 3H, H6, H5), 2.87 (t, J = 2.4 Hz, 1H, CH-propargyl), 2.01 (s, 3H, C(O)CH_3). **^{13}C NMR** (101 MHz, D_2O) δ 175.0 (C=O), 99.6 (C1), 78.7 (C_q-propargyl), 76.1 (CH-propargyl), 75.6 (C4), 74.5 (C5), 69.9 (C3), 60.9 (C6), 56.7 (CH_2-propargyl), 52.5 (C2), 22.2 (C(O)$\underline{C}H_3$). **HRMS** (ESI) m/z: [M + Na^+] calcd $C_{11}H_{16}NO_9SNa$ 384.0336, found 384.0338

2,3,3-trimethyl-3H-indole-5-sulfonic acid (13)

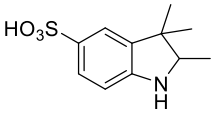

4-Hydrazinobenzenesulfonic acid (1.97 g, 10 mmol) was suspended in AcOH. 3-methyl-2-butanone (3 eqv., 2.58 g, 30 mmol) was added and the reaction mixture was refluxed for 3h. After cooling back to room temperature, the reaction mixture was triturated with EtOAc, the precipitate was collected by centrifugation and washed with cold EtOAc to give compound **13** as a pink powder (1.56 g, 6.5 mmol, 65%). **^{1}H NMR** (300 MHz, DMSO) δ 7.92 (d, *J* = 1.7 Hz, 1H), 7.87 (dd, *J* = 8.1, 1.7 Hz, 1H), 7.54 (d, *J* = 8.1 Hz, 1H), 1.43 (s, *J* = 7.2 Hz, 6H, C(CH_3)$_2$).

1,2,3,3-tetramethyl-3H-indol-1-ium-5-sulfonate (14)

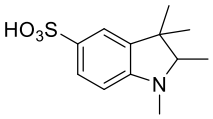

2,3,3-trimethyl-3H-indole-5-sulfonic acid (**13**) (0.550 g, 2.3 mmol) was dissolved in MeOH (11.5 mL). NaOAc (1.1 eqv., 0.205 g, 2.5 mmol) was added and the reaction mixture was stirred at RT for 15 min. The reaction mixture was concentrated under reduced pressure, co-evaporated with toluene (3x) and suspended in acetonitrile (11.5 mL). Iodomethane (2 eqv., 0.29 mL, 4.6 mmol) was added and the reaction mixture was stirred at 80°C for 22h. The reaction mixture was siluted by the addition of additional acetonitrile and the residue was obtained by decantation. This residue was washed three times with acetone to give compound **14** as a red solid (0.474 g, 1.9 mmol, 80%). **^{1}H NMR** (400 MHz, MeOD) δ 8.05 (d, *J* = 1.2 Hz, 1H, CH_{arom}), 7.96 (dd, *J* = 8.4, 1.2 Hz, 1H, CH_{arom}), 7.85 (d, *J* = 8.4 Hz, 1H, CH_{arom}), 4.08 (s, 3H, NCH_3), 1.61 (s, 6H, C(CH_3)$_2$).

1-(5-carboxypentyl)-2,3,3-trimethyl-3H-indol-1-ium-5-sulfonate (15)

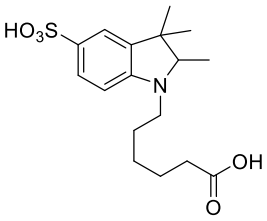

2,3,3-trimethyl-3H-indole-5-sulfonic acid (**13**) (0.718 g, 3 mmol) was dissolved in MeOH (12 mL). KOAc (1.1 eqv., 0.324 g, 3.3 mmol) was added and the reaction mixture was stirred at RT for 15 min. The reaction mixture was concentrated under reduced pressure, co-evaporated with toluene (3x) and suspended in 1,2-dichlorobenzene (12 mL). 6-bromohexanoic acid (1.25 eqv., 0.732 g, 3.75 mmol) was added and the reaction mixture was stirred at 110°C for 23h. The solvent was removed by decantation and the residue was washed 3 times with isopropanol to give compound **15** as a red powder (1.08 g, 3 mmol, quantitative). **^{1}H NMR** (400 MHz, MeOD) δ 8.13 (t, *J* = 4.5 Hz, 1H, CH_{arom}), 8.05 (dd, *J* = 8.4, 1.5 Hz, 1H, CH_{arom}), 7.96 – 7.89 (m, 1H, CH_{arom}), 4.53 (t, *J* = 4.5 Hz, 2H, $NC\underline{H}_2CH_2CH_2CH_2CH_2C(O)OH$), 2.37 – 2.27 (m, 2H, $NCH_2CH_2CH_2CH_2C\underline{H}_2C(O)OH$), 2.03 – 1.92 (m, 2H, $NCH_2C\underline{H}_2CH_2CH_2CH_2C(O)OH$), 1.77 – 1.65 (m, 4H, $NCH_2CH_2C\underline{H}_2C\underline{H}_2CH_2C(O)OH$), 1.62 (s, 6H, $C(CH_3)_2$).

Sulpho Cy5-OH (4)

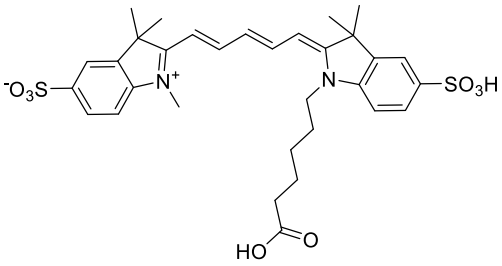

2,3,3-trimethyl-3H-indole-5-sulfonic acid (**14**) (0.999 g, 3.9 mmol) was dissolved in AcOH (20 mL) and Ac_2O (54 eqv., 20 mL, 210 mmol). Malonaldehyde bis(phenylimine) monohydrochloride (1.1 eqv., 1.11 g, 4.3 mmol) was added and the reaction mixture was refluxed for 4h. The reaction mixture was concentrated under reduced pressure, precipitated in EtOAc and washed 3 times with EtOAc to give the intermediate as a dark yellow solid (1.8 g, 3.9 mmol, quantitative). **LC-MS** RT = 4.7 min (C18, 10-90% B over 9 minutes) **LRMS** calcd $[M]^+$ = 425.15 observed M/z = 425.13

This intermediate (0,424 g, 1 mmol) and compound **15** (0.353 g, 1 mmol) were dissolved in pyridine (10 mL). Ac_2O (105 eqv., 10 mL, 105 mmol) was added and the reaction mixture was stirred at 110°C for 4h. The reaction mixture was triturated with EtOAc, the precipitate was collected by centrifugation and washed 3 times with isopropanol. Reverse phase HPLC yielded the title compound as dark blue solid (42 mg, 65 µmol, 7%). **^{1}H NMR** (400 MHz, D_2O) δ 7.85 (d, *J* = 12.4 Hz, 2H, C-CH=C$\underline{H}$-CH=C$\underline{H}$-CH=C), 7.74 (d, *J* = 5.1 Hz, 2H, aromatic), 7.73 – 7.68 (m, 2H, aromatic), 7.23 (dd, *J* = 8.3, 3.6 Hz, 2H, aromatic), 6.33 (t, *J* = 12.2 Hz, 1H, C-CH=CH-C$\underline{H}$=CH-CH=C), 3.98 – 3.88 (m, 2H, $NC\underline{H}_2CH_2CH_2CH_2CH_2C(O)OH$), 3.48 (s, 3H, NCH_3), 2.29 (t, *J* = 7.3 Hz, 2H, $NCH_2CH_2CH_2CH_2C\underline{H}_2C(O)OH$), 1.75 – 1.64 (m, 2H, $NCH_2C\underline{H}_2CH_2CH_2CH_2C(O)OH$), 1.60 – 1.48 (m, 14H, $NCH_2CH_2CH_2C\underline{H}_2CH_2C(O)OH$, 2x $C(CH_3)_2$), 1.41 – 1.28 (m, 2H, $NCH_2CH_2C\underline{H}_2CH_2CH_2C(O)OH$). **LC-MS** RT = 4.3 min (C18, 10-90% B over 9 minutes) **LRMS** calcd $[M]^+$ = 643.21 observed M/z = 643.33

SPPS procedures

General procedure for automated SPPS

Peptides were synthesized using automated Fmoc-SPPS on a Liberty Blue^{tm} automated microwave peptide synthesizer (CEM corporation). Synthesis was performed 100 µmol scale on Tentagel S RAM resin (loading 0.20-0.25 mmol/g, Rapp Polymere GmbH, Germany). Resin was first swollen for 5 minutes in DMF prior to amino acid coupling. Activation was achieved using DIC/Oxyma coupling as is

recommended by the manufacturer. The following amino acids were used: Fmoc-Ala-OH, Fmoc-Arg(Pbf)-OH, Fmoc-Asn(Trt)-OH, Fmoc-Asp(OtBu)-OH, Fmoc-Gln(tBu)-OH, Fmoc-Glu(OtBu), Fmoc-Gly-OH, Fmoc-Ile-OH, Fmoc-Leu-OH, Fmoc-Lys(Boc)-OH, Fmoc-Lys(Mmt)-OH, Fmoc-Phe-OH, Fmoc-Ser(tBu)-OH, Fmoc-Val-OH. All amino acids were obtained from Novabiochem except Fmoc-Lys(Mmt)-OH which was obtained from CEM corporation. Standard coupling was achieved using 5 equivalents amino acid as a 0.2 M amino acid/DMF solution, 5 equivalents DIC as a 0.5 M of DIC/DMF solution and 5 equivalents Oxyma as a 1 M Oxyma/DMF solution (also containing 0.2 M DiPEA), at 90°C for 2 minutes. Standard Fmoc deprotection was achieved by 20% (v/v) piperidine in DMF at 90°C for 90 seconds, repeated once. To analyze the quality of the peptide, a small amount of resin (~1mg) was treated with 200 µL of a TFA cocktail (95:2.5:2.5, TFA/H_2O/TIS) for 2 hours, after which the TFA was filtered into 800 µL of ice cold Et_2O. After five minutes the formed precipitate was collected by centrifugation and the supernatant discarded. The pellet was dissolved in 200 µL 1:1:1 H_2O/MeCN/tBuOH and subjected to LC-MS analysis. Peptides were characterized using electrospray ionization mass spectrometry (ESI-MS) on a Thermo Finnigan LCQ Advantage Max LC-MS instrument with a Surveyor PDA plus UV detector on an analytical C18 column (Phenomenex, 3 µm, 110 Å, 50 mm × 4.6 mm) in combination with buffers A (H_2O), B (MeCN), and C (1% aq TFA). Quality of crude was evaluated with a linear gradient of 10-90% B with a constant 10% C over 10 minutes.

General procedures for manual SPPS

Manual elongation of peptides was carried out in a fritted syringe at either 25 or 5 µmol scale. Fmoc deprotection was achieved using 20 % (v/v) piperidine in DMF in two steps, reacting 3 and 7 minutes respectively. Fmoc-Gly-OH was coupled using 5 equivalents of amino acid together with 5 equivalents of HCTU (as a 0.5 M solution) and 10 equivalents DiPEA for 45 minutes. Fmoc-Lys(N_3)-OH was coupled using 2 equivalents together with 2 equivalents HCTU (as a 0.2 M in DMF solution) and 4 equivalents of DiPEA for 90 minutes. Fmoc-TEG-OH (Chapter 5) was coupled using 4 equivalents, together with 4 equivalents HCTU and 8 equivalents DiPEA in 1 mL of DMF for 45 minutes. Analysis of the quality of the resin-bound peptide was carried out as above.

General procedure for N-terminal acetylation

The N-terminal Fmoc was cleaved by treating the resin twice with a 20% (v/v) solution of piperidine in DMF, for 3 and 7 minutes. This was followed by the addition of a solution containing 10 % (v/v) Ac_2O and 5 % (v/v) DiPEA in DMF (1 mL for 25 µmol resin bound peptide). This resin was acetylated for 15 minutes under gentle agitation, followed by draining the acetylation solution and thorough washing of the resin with DMF.

General procedure for fluorophore labeling

Fluorophore labeling of peptides was generally carried out on a 5 µmol scale. The resin was first swelled in DCM, followed by selective Mmt deprotection. The Mmt group protecting the C-terminal lysine residue, the resin was treated with a mildly acidic mixture consisting of 10 % (v/v) AcOH and 20 % (v/v) TFE in DCM (1 mL) for one hour.[33] After this time has elapsed, the resin was washed three times with DCM and three times with DMF. To remove residual acetic acid, the resin was then treated with a 10 % TEA in DMF mixture (2 x 10 min) followed by an additional three washes with DMF. One equivalent of fluorophore **16** was dissolved in a 50 mM solution of HCTU together with 2 equivalents of DiPEA. This mixture was added to the drained resin and allowed to react under gentle agitation overnight

protected from light. After overnight coupling the solution was drained and the resin was thoroughly washed with DMF.

General procedure for peptide global deprotection and purification

Peptide cleavage was carried out using a standard TFA cleavage cocktail (TFA:H_2O:TIS 95:2.5:2.5) using 1 mL per 25 µmol of resin bound peptide. Before initiating cleavage, the resin was thoroughly washed with DCM and drained. The TFA cocktail was added and mixed with the resin under gentle agitation for one hour, after which it was drained into a centrifuge tube containing ice cold diethyl ether (10:1 ratio Et_2O:TFA). When deprotecting fluorophore modified peptides, the cleavage reaction was protected from light as much as possible and a 20:1 ratio of Et_2O to TFA was used. The diethylether/TFA mixture was chilled for a minimum of 10 minutes to increase peptide recovery and the precipitated peptide was recovered by centrifugation. The supernatant was discarded and the pellet washed with a small amount of Et_2O, followed again by centrifugation. This pellet was dissolved in a mixture of H_2O/MeCN/tBuOH and subjected to RP-HPLC purification on a Gilson GX281 semipreparative HPLC. This machine was equipped with a Gemini-NX C18 column (5 µm, 110 A, 250 x 10.0 mm) using a flow of 5 mL/min and buffers A = 0.1% TFA in H_2O and B = MeCN. Peak detection was done using a UV-Vis detector set to 225 nm or 610 nm for fluorescently labeled peptides. Quality of purified peptides was determined using an electrospray ionization mass spectrometry (ESI-MS) on a Thermo Finnigan LCQ Advantage Max LC-MS instrument with a Surveyor PDA plus UV detector on an analytical C18 column (Phenomenex, 3 µm, 110 Å, 50 mm × 4.6 mm) in combination with buffers A (H_2O), B (MeCN), and C (1% aq TFA). Quality of the peptides was evaluated with a linear gradient of 10-50% B with a constant 10% C over 9 minutes or a linear gradient of 10-90% B with a constant 10% C over 9 minutes.

Fmoc-Asp(OtBu)-Glu(OtBu)-Val-Ser(tBu)-Gly-Leu-Glu(OtBu)-Gln(Trt)-Leu-Glu(OtBu)-Ser(tBu)-Ile-Ile-Asn(Trt)-Phe-Glu(OtBu)-Lys(Boc)-Leu-Ala-Ala-Ala-Ala-Ala-Lys(Mmt)-RAM-Tentagel S (16)

Peptide was synthesized on a 100 µmole scale using the general automated synthesis procedures. **LC-MS** RT = 5.3 min (C18, 10-90% B over 9 minutes) **LRMS** calcd $[M+2H]^{2+}$ = 1384.21, $[M+3H]^{3+}$ = 923.14 observed M/z = 1384.75, 923.50

Fmoc-Lys(N_3)-Gly-Asp(OtBu)-Glu(OtBu)-Val-Ser(tBu)-Gly-Leu-Glu(OtBu)-Gln(Trt)-Leu-Glu(OtBu)-Ser(tBu)-Ile-Ile-Asn(Trt)-Phe-Glu(OtBu)-Lys(Boc)-Leu-Ala-Ala-Ala-Ala-Ala-Lys(Mmt)-RAM-Tentagel S (17)

Resin bound peptide **16** (10 µmol) was elongated manually with Fmoc-Gly-OH and Fmoc-Lys(N_3)-OH. **LC-MS** RT = 5.6 min (C18, 10-90% B over 9 minutes) **LRMS** calcd $[M+2H]^{2+}$ = 1490.00, $[M+3H]^{3+}$ = 993.67 observed M/z = 1490.33, 994.08

Lys(N_3)-Gly-Asp-Glu-Val-Ser-Gly-Leu-Glu-Gln-Leu-Glu-Ser-Ile-Ile-Asn-Phe-Glu-Lys-Leu-Ala-Ala-Ala-Ala-Ala-Lys(sCy5)-NH_2 (20)

The C-terminal Lys(Mmt) of resin bound peptide **17** (10 µmol) was chemoselectively deprotected followed by coupling of **4** (1.0 eq, 6.4 mg, 10 µmol) as described in the general methods. Global deprotection followed by RP-HPLC purification yielded compound **20** as a blue solid (1.69 mg, 0.50 µmol, 5.0%). **LC-MS** RT = 7.2 min (C18, 10-50% B over 9 minutes) **LRMS** calcd $[M+2H]^{2+}$ = 1691.33, $[M+3H]^{3+}$ = 1127.88 observed M/z = 1691.25, 1128.17

Fmoc-Lys(N_3)-Lys(N_3)-Lys(N_3)-Lys(N_3)-Lys(N_3)-Lys(N_3)-Gly-Asp(OtBu)-Glu(OtBu)-Val-Ser(tBu)-Gly-Leu-Glu(OtBu)-Gln(Trt)-Leu-Glu(OtBu)-Ser(tBu)-Ile-Ile-Asn(Trt)-Phe-Glu(OtBu)-Lys(Boc)-Leu-Ala-Ala-Ala-Ala-Ala-Lys(Mmt)-RAM-Tentagel S (22)

Resin bound peptide **16** (25 µmol) was elongated manually with Fmoc-Gly-OH and Fmoc-Lys(N_3)-OH. **LC-MS** RT = 8.0 min (C18, 10-90% B over 9 minutes) **LRMS** calcd $[M+2H]^{2+}$ = 1875.48, $[M+3H]^{3+}$ = 1250.65 observed M/z = 1875.80, 1250.93

Lys(N_3)-Lys(N_3)-Lys(N_3)-Lys(N_3)-Lys(N_3)-Lys(N_3)-Gly-Asp-Glu-Val-Ser-Gly-Leu-Glu-Gln-Leu-Glu-Ser-Ile-Ile-Asn-Phe-Glu-Lys-Leu-Ala-Ala-Ala-Ala-Ala-Lys(sCy5)-NH_2 (24)

The C-terminal Lys(Mmt) of resin bound peptide **22** (5 µmol) was chemoselectively deprotected followed by coupling of **4** (1.0 eq, 3.2 mg, 5 µmol) as described in the general methods. Global deprotection followed by RP-HPLC purification yielded compound **24** as a blue solid (0.49 mg, 0.12 µmol, 2.4%). **LC-MS** RT = 5.4 min (C18, 10-90% B over 9 minutes) **LRMS** calcd $[M+3H]^{3+}$ = 1384.69 observed M/z = 1385.00

Ac-Lys(N_3)-Lys(N_3)-Lys(N_3)-Lys(N_3)-Lys(N_3)-Lys(N_3)-Gly-Asp-Glu-Val-Ser-Gly-Leu-Glu-Gln-Leu-Glu-Ser-Ile-Ile-Asn-Phe-Glu-Lys-Leu-Ala-Ala-Ala-Ala-Ala-Lys(sCy5)-NH_2 (28)

Resin bound peptide **22** (5 µmol) was N-terminally acetylated according to the standard conditions. This was followed by chemoselective deprotection of the Mmt group and coupling of **4** (1.0 eq, 3.2 mg, 5 µmol) as described in the general methods. Global deprotection followed by RP-HPLC purification yielded compound **28** as a blue solid (1.30 mg, 0.31 µmol, 6.2%). **LC-MS** RT = 6.4 min (C18, 10-90% B over 9 minutes) **LRMS** calcd $[M+3H]^{3+}$ = 1398.70 observed M/z = 1399.00

Fmoc-Lys(N_3)-Lys(N_3)-Lys(N_3)-Lys(N_3)-Lys(N_3)-Lys(N_3)-TEG-Asp(OtBu)-Glu(OtBu)-Val-Ser(tBu)-Gly-Leu-Glu(OtBu)-Gln(Trt)-Leu-Glu(OtBu)-Ser(tBu)-Ile-Ile-Asn(Trt)-Phe-Glu(OtBu)-Lys(Boc)-Leu-Ala-Ala-Ala-Ala-Ala-Lys(Mmt)-RAM-Tentagel S (31)

Resin bound peptide **16** (25 µmol) was elongated manually with Fmoc-TEG-OH and Fmoc-Lys(N_3)-OH. **LC-MS** RT = 7.6 min (C18, 10-90% B over 9 minutes) **LRMS** calcd $[M+2H]^{2+}$ = 1941.52, $[M+3H]^{3+}$ = 1294.68 observed M/z = 1941.53, 1294.80

Ac-Lys(N_3)-Lys(N_3)-Lys(N_3)-Lys(N_3)-Lys(N_3)-Lys(N_3)-TEG-Asp-Glu-Val-Ser-Gly-Leu-Glu-Gln-Leu-Glu-Ser-Ile-Ile-Asn-Phe-Glu-Lys-Leu-Ala-Ala-Ala-Ala-Ala-Lys(sCy5)-NH_2 (33)

Resin bound peptide **31** (5 µmol) was N-terminally acetylated according to the standard conditions. This was followed by chemoselective deprotection of the Mmt group and coupling of **4** (1.0 eq, 3.2 mg, 5 µmol) as described in the general methods. Global deprotection followed by RP-HPLC purification yielded compound **33** as a blue solid (1.60 mg, 0.37 µmol, 7.4%). **LC-MS** RT = 6.0 min (C18, 10-90% B over 9 minutes) **LRMS** calcd $[M+3H]^{3+}$ = 1443.06 observed M/z = 1443.00

Fmoc-Lys(N_3)-Gly-Lys(N_3)-TEG-Asp(OtBu)-Glu(OtBu)-Val-Ser(tBu)-Gly-Leu-Glu(OtBu)-Gln(Trt)-Leu-Glu(OtBu)-Ser(tBu)-Ile-Ile-Asn(Trt)-Phe-Glu(OtBu)-Lys(Boc)-Leu-Ala-Ala-Ala-Ala-Ala-Lys(Mmt)-RAM-Tentagel S (37)

Resin bound peptide **16** (25 µmol) was elongated manually with Fmoc-TEG-OH, Fmoc-Lys(N_3)-OH and Fmoc-Gly-OH. **LC-MS** RT = 6.5 min (C18, 10-90% B over 9 minutes) **LRMS** calcd $[M+2H]^{2+}$ = 1661.86, $[M+3H]^{3+}$ = 1108.24 observed M/z = 1662.00, 1108.67

Ac-Lys(N_3)-Gly-Lys(N_3)-TEG-Asp-Glu-Val-Ser-Gly-Leu-Glu-Gln-Leu-Glu-Ser-Ile-Ile-Asn-Phe-Glu-Lys-Leu-Ala-Ala-Ala-Ala-Ala-Lys(sCy5)-NH_2 (38)

Resin bound peptide **37** (5 µmol) was N-terminally acetylated according to the standard conditions. This was followed by chemoselective deprotection of the Mmt group and coupling of **4** (1.0 eq, 3.2 mg, 5 µmol) as described in the general methods. Global deprotection followed by RP-HPLC purification yielded compound **38** as a blue solid (1.24 mg, 0.33 µmol, 6.6%). **LC-MS** RT = 5.0 min (C18, 10-90% B over 9 minutes) **LRMS** calcd $[M+2H]^{2+}$ = 1883.93, $[M+3H]^{3+}$ = 1256.28 observed M/z = 1884.42, 1256.67

CuAAC glycopeptide conjugation

General procedures for CuAAC modification of peptides

Peptides were dissolved in degassed DMSO and glycans in either degassed DMSO or degassed MilliQ water. These were mixed together in a 1.5 mL Eppendorf tube, followed by addition of a copper click mix. This click mix typically consistent of 1 part 0.1 M $CuSO_4$ (in MQ), 2 parts 0.1 M sodium ascorbate (in MQ) and 3 parts 0.1 M THPTA (in DMSO), giving a solution with a total Cu(I) concentration of around 15 mM. Of this solution, enough was added to be 0.15 equivalents compared to the peptide. The reaction was heated in a 40°C shaker block, and every 24 hours 1 equivalent of 0.1 M sodium ascorbate was added. Periodically, a 0.5 µL sample was diluted into 39.5 µL of 1:1:1 H_2O/MeCN/tBuOH and analyzed by LC-MS to evaluate reaction progression. After full conversion of the peptide towards the desired conjugate was observed, the reaction mixture was subjected to size exclusion chromatography over Toyopearl HW-40 size exclusion resin using 150 mM NH_4OAc or 150 mM NH_4HCO_3 (containing 20% MeCN) as the buffer. Fractions showing absorbance at 610 nm were combined and lyophilized.

Lys(4-SO_4-GalNAc)-Gly-Asp-Glu-Val-Ser-Gly-Leu-Glu-Gln-Leu-Glu-Ser-Ile-Ile-Asn-Phe-Glu-Lys-Leu-Ala-Ala-Ala-Ala-Ala-Lys(sCy5)-NH_2 (21)

Compound **20** (0.5 µmol) was dissolved in 15 µl degassed DMSO and sugar **3** was added (2 eq., 10 µL of 0.1 M solution in H_2O). A click mix was prepared by mixing CuI (1 eq, 0.1 M), THPTA (3 eq, 0.3 M) and DiPEA (2 eq, 0.2 M) and 1 µL of this mixture was added to the reaction mix. After SEC purification and lyophilization compound **21** was obtained as a blue powder (1.37 mg, 0.37 µmol, 74%). **LC-MS** RT = 7.0 min (C18, 10-50% B over 9 minutes) **LRMS** calcd $[M+2H]^{2+}$ = 1860.86, $[M+3H]^{3+}$ = 1240.93 observed M/z = 1860.83, 1240.92

Lys(Man)-Lys(Man)-Lys(Man)-Lys(Man)-Lys(Man)-Lys(Man)-Gly-Asp-Glu-Val-Ser-Gly-Leu-Glu-Gln-Leu-Glu-Ser-Ile-Ile-Asn-Phe-Glu-Lys-Leu-Ala-Ala-Ala-Ala-Ala-Lys(sCy5)-NH_2 (25)

Compound **24** (50 nmol, 5 mM in DMSO) was mixed with propargyl mannoside **1** (7.5 eq., 7.5 µL of 50 mM solution in 1:1 H_2O/DMSO). 0.5 µL of the standard click mix was added and the reaction carried out at 40°C. After SEC purification and lyophilization compound **25** was obtained as a blue powder (0.67 mg). **LC-MS** RT = 6.7 min (C18, 10-50% B over 9 minutes) **LRMS** calcd $[M+3H]^{3+}$ = 1821.19, $[M+4H]^{4+}$ = 1366.14 observed M/z = 1821.00, 1366.08

Ac-Lys(Man)-Lys(Man)-Lys(Man)-Lys(Man)-Lys(Man)-Lys(Man)-Gly-Asp-Glu-Val-Ser-Gly-Leu-Glu-Gln-Leu-Glu-Ser-Ile-Ile-Asn-Phe-Glu-Lys-Leu-Ala-Ala-Ala-Ala-Ala-Lys(sCy5)-NH_2 (29)

Compound **28** (100 nmol, 50 mM in DMSO) was mixed with propargyl mannoside **1** (12 eq., 6 µL of 200 mM solution in 1:1 H_2O/DMSO). 1 µL of the standard click mix was added and the reaction carried out

at 40°C. After SEC purification and lyophilization compound **29** was obtained as a blue powder (0.11 mg, 20 nmol, 20%). **LC-MS** RT = 6.7 min (C18, 10-50% B over 9 minutes) **LRMS** calcd $[M+3H]^{3+}$ = 1835.22, $[M+4H]^{4+}$ = 1376.67 observed M/z = 1835.25, 1376.92

Ac-Lys(Man)-Lys(Man)-Lys(Man)-Lys(Man)-Lys(Man)-Lys(Man)-TEG-Asp-Glu-Val-Ser-Gly-Leu-Glu-Gln-Leu-Glu-Ser-Ile-Ile-Asn-Phe-Glu-Lys-Leu-Ala-Ala-Ala-Ala-Ala-Lys(sCy5)-NH_2 (34)

Compound **33** (100 nmol, 50 mM in DMSO) was mixed with propargyl mannoside **1** (12 eq., 6 µL of 200 mM solution in DMSO). 1 µL of the standard click mix was added and the reaction carried out at 40°C. After SEC purification and lyophilization compound **34** was obtained as a blue powder (0.48 mg, 85 nmol, 85%). **LC-MS** RT = 4.3 min (C18, 10-50% B over 9 minutes) **LRMS** calcd $[M+3H]^{3+}$ = 1879.21, $[M+4H]^{4+}$ = 1409.66 observed M/z = 1879.33, 1409.83

Ac-Lys(triMan)-Lys(triMan)-Lys(triMan)-Lys(triMan)-Lys(triMan)-Lys(triMan)-TEG-Asp-Glu-Val-Ser-Gly-Leu-Glu-Gln-Leu-Glu-Ser-Ile-Ile-Asn-Phe-Glu-Lys-Leu-Ala-Ala-Ala-Ala-Ala-Lys(sCy5)-NH_2 (35)

Compound **34** (100 nmol, 50 mM in DMSO) was mixed with propargyl mannoside **2** (12 eq., 6 µL of 200 mM solution in DMSO). 1 µL of the standard click mix was added and the reaction carried out at 40°C. After SEC purification and lyophilization compound **35** was obtained as a blue powder (0.41 mg, 54 nmol, 54%). **LC-MS** RT = 4.2 min (C18, 10-50% B over 9 minutes) **LRMS** calcd $[M+4H]^{4+}$ = 1896.07, $[M+5H]^{5+}$ = 1517.06 observed M/z = 1896.08, 1517.17

Ac-Lys(Man)-Gly-Lys(Man)-TEG-Asp-Glu-Val-Ser-Gly-Leu-Glu-Gln-Leu-Glu-Ser-Ile-Ile-Asn-Phe-Glu-Lys-Leu-Ala-Ala-Ala-Ala-Ala-Lys(sCy5)-NH_2 (39)

Compound **38** (100 nmol, 25 mM in DMSO) was mixed with propargyl mannoside **1** (4 eq., 2 µL of 200 mM solution in DMSO). 1 µL of the standard click mix was added and the reaction carried out at 40°C. After SEC purification and lyophilization compound **39** was obtained as a blue powder (0.25 mg, 60 nmol, 60%). **LC-MS** RT = 6.8 min (C18, 10-50% B over 9 minutes) **LRMS** calcd $[M+3H]^{3+}$ = 1402.00 observed M/z = 1402.08

Ac-Lys(triMan)-Gly-Lys(triMan)-TEG-Asp-Glu-Val-Ser-Gly-Leu-Glu-Gln-Leu-Glu-Ser-Ile-Ile-Asn-Phe-Glu-Lys-Leu-Ala-Ala-Ala-Ala-Ala-Lys(sCy5)-NH_2 (40)

Compound **38** (100 nmol, 25 mM in DMSO) was mixed with propargyl mannoside **2** (4 eq., 2 µL of 200 mM solution in DMSO). 1 µL of the standard click mix was added and the reaction carried out at 40°C. After SEC purification and lyophilization compound **40** was obtained as a blue powder (0.29 mg, 60 nmol, 60%). **LC-MS** RT = 6.6 min (C18, 10-50% B over 9 minutes) **LRMS** calcd $[M+3H]^{3+}$ = 1618.07 observed M/z = 1618.08

Ac-Lys(4-SO_4-GalNAc)-Gly-Lys(4-SO_4-GalNAc)-TEG-Asp-Glu-Val-Ser-Gly-Leu-Glu-Gln-Leu-Glu-Ser-Ile-Ile-Asn-Phe-Glu-Lys-Leu-Ala-Ala-Ala-Ala-Ala-Lys(sCy5)-NH_2 (41)

Compound **38** (100 nmol, 25 mM in DMSO) was mixed with propargyl N-acetylgalactosamine **3** (4 eq., 2 µL of 200 mM solution in DMSO). 1 µL of the standard click mix was added and the reaction carried out at 40°C. After SEC purification and lyophilization compound **41** was obtained as a blue powder (0.23 mg, 52 nmol, 52%). **LC-MS** RT = 6.8 min (C18, 10-50% B over 9 minutes) **LRMS** calcd $[M+3H]^{3+}$ = 1482.66 observed M/z = 1482.67

Glyco-PAINT data acquisition and analysis

CHO-MR and wt CHO cells were cultured as described previously.[19] Image acquisition was carried out on a NIKON Ti-2 microscope in a 512 x 512 pixel region (pixel dimensions: 0.160 µm x 0.160 µm). At least 5000 frames were collected using a 50 ms acquisition time. A 640 nm laser at 40 mW was used to illuminate the fluorescent molecules.

Data analysis was carried out using the open source Fiji package. First, individual fluorescent puncta were detected using the LoG (Laplacian of Gaussian) detector of the TrackMate plug-in, with the estimated object diameter set to 0.480 µm and median filter preprocessing turned on. Next, these detected puncta were tracked over time using the 'simple LAP tracker' option, with 'linking max distance' and 'gap-closing max distance' set to 0.6 µm and 'gap-closing max frame gap' set to 3. From the resulting tracks, only tracks containing > 3 individual spots were included for further analysis. Heatmaps were generated from 5000 frames analyzed over the whole image. The average position of every track was rounded down on both the x and y axis, effectively binning events per μm^2. The resulting track density was plotted as a 2D histogram using matplotlib.

References

(1) Rudd, P. M.; Elliott, T.; Cresswell, P.; Wilson, I. A.; Dwek, R. A. Glycosylation and the Immune System. *Science* **2001**, *291* (5512), 2370–2376. https://doi.org/10.1126/science.291.5512.2370.

(2) Torigoe, S.; Schutt, C. R.; Yamasaki, S. Immune Discrimination of the Environmental Spectrum through C-Type Lectin Receptors. *Int. Immunol.* **2021**, *33* (12), 847–851. https://doi.org/10.1093/intimm/dxab074.

(3) Rabinovich, G. A.; van Kooyk, Y.; Cobb, B. A. Glycobiology of Immune Responses. *Ann. N. Y. Acad. Sci.* **2012**, *1253* (1), 1–15. https://doi.org/10.1111/J.1749-6632.2012.06492.X.

(4) Nigou, J.; Zelle-Rieser, C.; Gilleron, M.; Thurnher, M.; Puzo, G. Mannosylated Lipoarabinomannans Inhibit IL-12 Production by Human Dendritic Cells: Evidence for a Negative Signal Delivered Through the Mannose Receptor. *J. Immunol.* **2001**, *166* (12), 7477–7485. https://doi.org/10.4049/JIMMUNOL.166.12.7477.

(5) Gringhuis, S. I.; den Dunnen, J.; Litjens, M.; van der Vlist, M.; Geijtenbeek, T. B. H. Carbohydrate-Specific Signaling through the DC-SIGN Signalosome Tailors Immunity to Mycobacterium Tuberculosis, HIV-1 and Helicobacter Pylori. *Nat. Immunol.* **2009**, *10* (10), 1081–1088. https://doi.org/10.1038/ni.1778.

(6) Denda-Nagai, K.; Aida, S.; Saba, K.; Suzuki, K.; Moriyama, S.; Oo-puthinan, S.; Tsuiji, M.; Morikawa, A.; Kumamoto, Y.; Sugiura, D.; Kudo, A.; Akimoto, Y.; Kawakami, H.; Bovin, N. V.; Irimura, T. Distribution and Function of Macrophage Galactose-Type C-Type Lectin 2 (MGL2/CD301b): Efficient Uptake and Presentation of Glycosylated Antigens by Dendritic Cells. *J. Biol. Chem.* **2010**, *285* (25), 19193–19204. https://doi.org/10.1074/jbc.M110.113613.

(7) Martinez-Pomares, L. The Mannose Receptor. *J. Leukoc. Biol.* **2012**, *92* (6), 1177–1186. https://doi.org/10.1189/JLB.0512231.

(8) East, L.; Isacke, C. M. The Mannose Receptor Family. *Biochim. Biophys. Acta - Gen. Subj.* **2002**, *1572* (2–3), 364–386. https://doi.org/10.1016/S0304-4165(02)00319-7.

(9) Mullin, N. P.; Hall, K. T.; Taylor, M. E. Characterization of Ligand Binding to a Carbohydrate-Recognition Domain of the Macrophage Mannose Receptor. *J. Biol. Chem.* **1994**, *269* (45), 28405–28413. https://doi.org/10.1016/s0021-9258(18)46942-6.

(10) Taylor, M. E.; Drickamer, K. Structural Requirements for High Affinity Binding of Complex Ligands by the Macrophage Mannose Receptor. *J. Biol. Chem.* **1993**, *268* (1), 399–404. https://doi.org/10.1016/S0021-9258(18)54164-8.

(11) Feinberg, H.; Jégouzo, S. A. F.; Lasanajak, Y.; Smith, D. F.; Drickamer, K.; Weis, W. I.; Taylor, M. E. Structural Analysis of Carbohydrate Binding by the Macrophage Mannose Receptor CD206. *J. Biol. Chem.* **2021**, *296*, 100368–100369. https://doi.org/10.1016/j.jbc.2021.100368.

(12) Napper, C. E.; Drickamer, K.; Taylor, M. E. Collagen Binding by the Mannose Receptor Mediated through the Fibronectin Type II Domain. *Biochem. J.* **2006**, *395* (3), 579–586. https://doi.org/10.1042/BJ20052027.

(13) Leteux, C.; Chai, W.; Loveless, R. W.; Yuen, C. T.; Uhlin-Hansen, L.; Combarnous, Y.; Jankovic, M.; Maric, S. C.; Misulovin, Z.; Nussenzweig, M. C.; Feizi, T. The Cysteine-Rich Domain of the Macrophage Mannose Receptor Is a Multispecific Lectin That Recognizes Chondroitin Sulfates a and B and Sulfated Oligosaccharides of Blood Group Lewisa and Lewisx Types in Addition to the Sulfated N-Glycans of Lutropin. *J. Exp. Med.* **2000**, *191* (7), 1117–1126. https://doi.org/10.1084/JEM.191.7.1117.

(14) Burgdorf, S.; Kautz, A.; Böhnert, V.; Knolle, P. A.; Kurts, C. Distinct Pathways of Antigen Uptake and Intracellular Routing in CD4 and CD8 T Cell Activation. *Science* **2007**, *316* (5824), 612–616. https://doi.org/10.1126/science.1137971.

(15) Butler, N. S.; Nolz, J. C.; Harty, J. T. Immunologic Considerations for Generating Memory CD8 T Cells through Vaccination. *Cell. Microbiol.* **2011**, *13* (7), 925–933. https://doi.org/10.1111/J.1462-5822.2011.01594.X.

(16) Ott, P. A.; Hu, Z.; Keskin, D. B.; Shukla, S. A.; Sun, J.; Bozym, D. J.; Zhang, W.; Luoma, A.; Giobbie-Hurder, A.; Peter, L.; Chen, C.; Olive, O.; Carter, T. A.; Li, S.; Lieb, D. J.; Eisenhaure, T.; Gjini, E.; Stevens, J.; Lane, W. J.; Javeri, I.; Nellaiappan, K.; Salazar, A. M.; Daley, H.; Seaman, M.; Buchbinder, E. I.; Yoon, C. H.; Harden, M.; Lennon, N.; Gabriel, S.; Rodig, S. J.; Barouch, D. H.; Aster, J. C.; Getz, G.; Wucherpfennig, K.; Neuberg, D.; Ritz, J.; Lander, E. S.; Fritsch, E. F.; Hacohen, N.; Wu, C. J. An Immunogenic Personal Neoantigen Vaccine for Patients with Melanoma. *Nature* **2017**, *547* (7662), 217–221. https://doi.org/10.1038/nature22991.

(17) Rauen, J.; Kreer, C.; Paillard, A.; Van Duikeren, S.; Benckhuijsen, W. E.; Camps, M. G.; Valentijn, A. R. P. M.; Ossendorp, F.; Drijfhout, J. W.; Arens, R.; Burgdorf, S. Enhanced Cross-Presentation and Improved CD8+ T Cell Responses after Mannosylation of Synthetic Long Peptides in Mice. *PLoS One* **2014**, *9* (8), e103755. https://doi.org/10.1371/journal.pone.0103755.

(18) McIntosh, J. D.; Brimble, M. A.; Brooks, A. E. S.; Dunbar, P. R.; Kowalczyk, R.; Tomabechi, Y.; Fairbanks, A. J. Convergent Chemo-Enzymatic Synthesis of Mannosylated Glycopeptides; Targeting of Putative Vaccine Candidates to Antigen Presenting Cells. *Chem. Sci.* **2015**, *6* (8), 4636–4642. https://doi.org/10.1039/c5sc00952a.

(19) Riera, R.; Hogervorst, T. P.; Doelman, W.; Ni, Y.; Pujals, S.; Bolli, E.; Codée, J. D. C.; van Kasteren, S. I.; Albertazzi, L. Single-Molecule Imaging of Glycan–Lectin Interactions on Cells with Glyco-PAINT. *Nat. Chem. Biol.* **2021**, *17* (12), 1281–1288. https://doi.org/10.1038/s41589-021-00896-2.

(20) Rosalia, R. A.; Quakkelaar, E. D.; Redeker, A.; Khan, S.; Camps, M.; Drijfhout, J. W.; Silva, A. L.; Jiskoot, W.; Hall, T. van; Veelen, P. A. van; Janssen, G.; Franken, K.; Cruz, L. J.; Tromp, A.; Oostendorp, J.; Burg, S. H. van der; Ossendorp, F.; Melief, C. J. M. Dendritic Cells Process Synthetic Long Peptides Better than Whole Protein, Improving Antigen Presentation and T-Cell Activation. *Eur. J. Immunol.* **2013**, *43* (10), 2554–2565. https://doi.org/10.1002/EJI.201343324.

(21) Gential, G. P. P.; Hogervorst, T. P.; Tondini, E.; van de Graaff, M. J.; Overkleeft, H. S.; Codée, J. D. C.; van der Marel, G. A.; Ossendorp, F.; Filippov, D. V. Peptides Conjugated to 2-Alkoxy-8-Oxo-Adenine as Potential Synthetic Vaccines Triggering TLR7. *Bioorg. Med. Chem. Lett.* **2019**, *29* (11), 1340–1344. https://doi.org/10.1016/J.BMCL.2019.03.048.

(22) Reintjens, N. R. M.; Tondini, E.; De Jong, A. R.; Meeuwenoord, N. J.; Chiodo, F.; Peterse, E.; Overkleeft, H. S.; Filippov, D. V.; Van Der Marel, G. A.; Ossendorp, F.; Codée, J. D. C. Self-Adjuvanting Cancer Vaccines from Conjugation-Ready Lipid A Analogues and Synthetic Long Peptides. *J. Med. Chem.* **2020**, *63* (20), 11691–11706. https://doi.org/10.1021/acs.jmedchem.0c00851.

(23) Reintjens, N. R. M. M.; Tondini, E.; Vis, C.; McGlinn, T.; Meeuwenoord, N. J.; Hogervorst, T. P.; Overkleeft, H. S.; Filippov, D. V.; Marel, G. A. van der; Ossendorp, F.; Codée, J. D. C. C.; van der Marel, G. A.; Ossendorp, F.; Codée, J. D. C. C. Multivalent, Stabilized Mannose-6-Phosphates for the Targeted Delivery of Toll-Like Receptor Ligands and Peptide Antigens. *ChemBioChem* **2021**, *22* (2), 434–440. https://doi.org/10.1002/CBIC.202000538.

(24) Liu, Y.; Chirino, A. J.; Misulovin, Z.; Leteux, C.; Feizi, T.; Nussenzweig, M. C.; Bjorkman, P. J. Crystal Structure of the Cysteine-Rich Domain of Mannose Receptor Complexed with a Sulfated Carbohydrate Ligand. *J. Exp. Med.* **2000**, *191* (7), 1105–1116.

https://doi.org/10.1084/JEM.191.7.1105.

(25) Liu, Y.; Misulovin, Z.; Bjorkman, P. J. The Molecular Mechanism of Sulfated Carbohydrate Recognition by the Cysteine-Rich Domain of Mannose Receptor. *J. Mol. Biol.* **2001**, *305* (3), 481–490. https://doi.org/10.1006/JMBI.2000.4326.

(26) Li, H.; Vaughan, J. C. Switchable Fluorophores for Single-Molecule Localization Microscopy. *Chemical Reviews*. American Chemical Society September 26, 2018, pp 9412–9454. https://doi.org/10.1021/acs.chemrev.7b00767.

(27) Mujumdar, R. B.; Ernst, L. A.; Mujumdar, S. R.; Lewis, C. J.; Waggoner, A. S. Cyanine Dye Labeling Reagents: Sulfoindocyanine Succinimidyl Esters. *Bioconjug. Chem.* **2002**, *4* (2), 105–111. https://doi.org/10.1021/BC00020A001.

(28) Rising, T. W. D. F.; Claridge, T. D. W.; Davies, N.; Gamblin, D. P.; Moir, J. W. B.; Fairbanks, A. J. Synthesis of N-Glycan Oxazolines: Donors for Endohexosaminidase Catalysed Glycosylation. *Carbohydr. Res.* **2006**, *341* (10), 1574–1596. https://doi.org/10.1016/j.carres.2006.03.007.

(29) Oscarson, S.; Tidén, A. K. Syntheses of the Octyl and Tetradecyl Glycosides of 3,6-Di-O-α-d-Mannopyranosyl-α-d-Mannopyranose and of 3,4-Di-O-α-d-Mannopyranosyl-α-d-Mannopyranose. A New Way for 2,4-Di-O-Protection of Mannopyranosides. *Carbohydr. Res.* **1993**, *247* (C), 323–328. https://doi.org/10.1016/0008-6215(93)84266-9.

(30) Andersen, S. M.; Heuckendorff, M.; Jensen, H. H. 3-(Dimethylamino)-1-Propylamine: A Cheap and Versatile Reagent for Removal of Byproducts in Carbohydrate Chemistry. *Org. Lett.* **2015**, *17* (4), 944–947. https://doi.org/10.1021/acs.orglett.5b00041.

(31) Christensen, H.; Christiansen, M. S.; Petersen, J.; Jensen, H. H. Direct Formation of β-Glycosides of N-Acetyl Glycosamines Mediated by Rare Earth Metal Triflates. *Org. Biomol. Chem.* **2008**, *6* (18), 3276–3283. https://doi.org/10.1039/b807064d.

(32) Weerapana, E.; Glover, K. J.; Chen, M. M.; Imperiali, B. Investigating Bacterial N-Linked Glycosylation: Synthesis and Glycosyl Acceptor Activity of the Undecaprenyl Pyrophosphate-Linked Bacillosamine. *J. Am. Chem. Soc.* **2005**, *127* (40), 13766–13767. https://doi.org/10.1021/ja054265v.

(33) Aletras, A.; Barlos, K.; Gatos, D.; Koutsogianni, S.; MAMOS, P. Preparation of the Very Acid-sensitive Fmoc-Lys(Mtt)-OH Application in the Synthesis of Side-chain to Side-chain Cyclic Peptides and Oligolysine Cores Suitable for the Solid-phase Assembly of MAPs and TASPs. *Int. J. Pept. Protein Res.* **1995**, *45* (5), 488–496. https://doi.org/10.1111/j.1399-3011.1995.tb01065.x.

(34) Hong, V.; Presolski, S. I.; Ma, C.; Finn, M. G. Analysis and Optimization of Copper-Catalyzed Azide-Alkyne Cycloaddition for Bioconjugation. *Angew. Chem. Int. Ed.* **2009**, *48* (52), 9879–9883. https://doi.org/10.1002/anie.200905087.

(35) Moorman, R. M.; Collier, M. B.; Frohock, B. H.; Womble, M. D.; Chalker, J. M. Halide Inhibition of the Copper-Catalysed Azide–Alkyne Cycloaddition. *Org. Biomol. Chem.* **2015**, *13* (7), 1974–1978. https://doi.org/10.1039/C4OB02479F.

(36) Li, R. J. E.; Hogervorst, T. P.; Achilli, S.; Bruijns, S. C.; Arnoldus, T.; Vivès, C.; Wong, C. C.; Thépaut, M.; Meeuwenoord, N. J.; van den Elst, H.; Overkleeft, H. S.; van der Marel, G. A.; Filippov, D. V.; van Vliet, S. J.; Fieschi, F.; Codée, J. D. C.; van Kooyk, Y. Systematic Dual Targeting of Dendritic Cell C-Type Lectin Receptor DC-SIGN and TLR7 Using a Trifunctional Mannosylated Antigen. *Front. Chem.* **2019**, *7*, 650. https://doi.org/10.3389/fchem.2019.00650.

(37) Tinevez, J. Y.; Perry, N.; Schindelin, J.; Hoopes, G. M.; Reynolds, G. D.; Laplantine, E.; Bednarek, S. Y.; Shorte, S. L.; Eliceiri, K. W. TrackMate: An Open and Extensible Platform for Single-Particle

Tracking. *Methods* **2017**, *115*, 80–90. https://doi.org/10.1016/J.YMETH.2016.09.016.

(38) Patel, M. K.; Vijayakrishnan, B.; Koeppe, J. R.; Chalker, J. M.; Doores, K. J.; Davis, B. G. Analysis of the Dispersity in Carbohydrate Loading of Synthetic Glycoproteins Using MALDI-TOF Mass Spectrometry. *Chem. Commun.* **2010**, *46* (48), 9119–9121. https://doi.org/10.1039/c0cc03420g.

(39) Wong, C. S.; Hoogendoorn, S.; Van Der Marel, G. A.; Overkleeft, H. S.; Codée, J. D. C. Targeted Delivery of Fluorescent High-Mannose-Type Oligosaccharide Cathepsin Inhibitor Conjugates. *Chempluschem* **2015**, *80* (6), 928–937. https://doi.org/10.1002/CPLU.201500004.

(40) Wipf, P.; Eyer, B. R.; Yamaguchi, Y.; Zhang, F.; Neal, M. D.; Sodhi, C. P.; Good, M.; Branca, M.; Prindle, T.; Lu, P.; Brodsky, J. L.; Hackam, D. J. Synthesis of Anti-Inflammatory α-and β-Linked Acetamidopyranosides as Inhibitors of Toll-like Receptor 4 (TLR4). *Tetrahedron Lett.* **2015**, *56* (23), 3097–3100. https://doi.org/10.1016/J.TETLET.2014.11.048.